博士論文

題 目

LTD 型パルスパワー発生器の特性評価と
これを用いた大気圧放電研究

LTD-Type Pulsed Power Generator and Its
Applications to Atmospheric Pressure Discharge

著者
KAZEMI MOHAMMAD REZA
(12507081)

指導教員
江　偉華　教授

長岡技術科学大学工学部
エネルギー・環境工学専攻

平成 **29** 年 **6** 月

論　文　内　容　の　要　旨

氏　名　　Kazemi Mohammad Reza

本論文は、「LTD 型パルスパワー発生器の特性評価とこれを用いた大気圧放電研究」と題し、5 章より構成されている。第 1 章では、研究の背景、問題の特定、研究の目的を概説する。パルス電力発生方法が示されており、パルス電力エネルギーの潜在的な用途の一つとして、大気圧放電を導入する。
第 2 章では、コンパクトなパルス発生器である Linear Transformer Driver（LTD）について説明する。 LTD のコンセプト、回路や構造が示されている。また、Field Programmable Gate Array（FPGA）が LTD 制御信号源として選択された理由について説明した。
第 3 章では、FPGA と LTD を組み合わせたシステムの柔軟性を示すいくつかの実験が行われている。 このシステムを用い、LTD の各段に FPGA から任意の制御信号を供給することにより、負荷に任意の出力が可能であることが示されている。実験的なセットアップと結果が示されている。
第 4 章では、パルス型大気放電の波形を制御するために LTD を使用した。この種の放電負荷は、インピーダンスが変化するため、通常、一定電圧では一定の電流が得られないことが知られている。それは、一定の振幅の電圧が印加され続けると、放電プラズマが広がり、電極間に低インピーダンスのチャネルが急速に形成され、放電電流が大幅に増加するからである。現在は、このインピーダンスの変動を回避するために、電圧の印加を終了させ、電流が制御不能になる前にパルスを終える方法が最も一般的です。そこで我々は、LTD の制御信号を FPGA を用いて調整し、LTD の充電電圧を変更することなく、印加電圧を変化させることでこの問題に対応した。
実験結果は、印加電圧を適切に調整することによって放電負荷の電流をある程度制御できることを証明している。
パルス幅が 100ns で電流の振幅が 40A、30A、20A、10A とそれぞれ一定のパルスを生成することができた。また、同様の方法で電流のステップアップ（10A→30A）やステップダウン（30A→10A）の試験を行った。その結果、ステップアップやステップダウンで任意に電流を制御することができました。この電流波形制御技術は、放電生成プラズマの様々な用途に重大な意味を持つと考えられる。
第 5 章では、本研究室の LTD 型パルス電圧発生器を使用して、パルス大気放電の影響を知るために、連続運転での挙動を調査した。パルス大気放電への適用には反復動作を必要とし、パルス放電はガス中に発生するため、それに続く次のパルスでは異なる挙動をもたらすことを知り、理解することは常に重要である。
LTD の出力柔軟性を利用して、ワイヤーとパイプからなる同軸放電負荷に連続した 2 つのパルスを印加してガス放電挙動を調べた。実験結果は、2 つのパルスが互いに近すぎる（<100 μ s）場合に、第 2 のパルスの放電電流が電圧振幅が一定であるにも関わらず、第 1 のパルスの放電電流よりも低いことを示している。

この効果を物理的に説明するために、我々は、最初の放電によってガス中に生成されて散在する残留正電荷の影響を検討した。電場分布を解くために 1 次元モデルを構築した。計算結果は、残留電荷が考慮されたときの電場の著しい低下を示しており、実験結果を定性的に説明することができる。即ち、第 1 のパルス放電は、第 2 のパルス電圧が印加されたときに電界を弱める役割を果たす正電荷をガス中に残してしまうと物理的に解釈することができる。この研究によって得られた知見は、パルス大気放電の基本的な特性を理解するのに役立つと考えられる。よって、本論文は工学上及び工業上貢献するところが大きく、博士（工学）の学位論文として十分な価値を有するものと認める。

ABSTRACT

Chapter 1 as introduction outlines the research background, problem identification and research objectives. Pulsed Power generation method has been shown and Atmospheric pressure discharge as one of the potential applications of pulsed power energy has introduced. Chapter 2 talks about Linear Transformer Driver (LTD) as a compact Pulsed Power Generator. LTD concept, Circuit and Structure haven been shown. It has been explained that why Field Programmable Gate Array (FPGA) has been selected as LTD control signal source. In chapter 3, FPGA and LTD combined system have been used for some experiments to show the flexibility of this system. Different type of control signals provided by FPGA has been delivered to LTD. It has been shown that by providing proper control signals we can have arbitrary output in the load. Experimental setup and result has been shown. In chapter 4, we used our LTD to control the waveform of Pulsed Atmospheric Discharge. This kind of discharge load is known for its time-varying impedance where constant voltage usually does not result in constant current. If the applied voltage amplitude is sustained, it will expand the discharge plasma and quickly form a low impedance channel between the electrodes and discharge current increases significantly. So far, the most typical way of avoiding this impedance collapse is to terminate the applied voltage and finish the pulse before the current gets out of control. We manually adjusted the LTD control signals through FPGA without changing LTD charging voltage to change the applied voltage. The experimental results have proved that the current of a discharge load can be arbitrarily controlled, to a certain extent, by properly adjusting the applied voltage. We could keep the current amplitude in certain

values of 40, 30, 20, 10 A with pulse width of 100 ns. We also demonstrated the current drawing by this method. We could control the current arbitrarily in a step up and step down manner. This kind of current waveform control should have significant implications for various applications of discharge-generated plasmas. In chapter 5, we have used our LTD-type pulsed voltage generator to study the influence of a pulsed atmospheric discharge on the behavior of the following pulse for consecutive operation. Since applications of pulsed atmospheric discharge require repetitive operation, it is always important to know and to understand the effect a pulsed discharge can create in the gas that may result in different behavior of the next pulse following it. Taking advantage of the output flexibility of the LTD, we have studied gas discharge behavior by applying two consecutive pulses to a coaxial discharge load consisting of a wire and a pipe. The experimental results have shown that the discharge current of the second pulse is always lower than that of the first pulse for the same voltage amplitude, when the two pulses are too close to each other (< 100 μs). In order to provide a physical interpretation of this effect, we have looked into the influence of residual positive charge that is created and littered in the gas by the first discharge. A one-dimensional model has been built in order to solve for the electric field distribution. The calculation results have indicated a significant drop of the electric field when the residual charge has been taken into account, offering a qualitative explanation for the experimental results. In other words, it can be physically interpreted that the first pulsed discharge has left some positive charge in the gas that plays a role in weakening the electric field when the second pulsed voltage is applied. The findings obtained by this study will help us understand the fundamental characteristics of pulsed atmospheric discharge.

AKCNOWLEDGMENT

Foremost, I would like to express my sincere gratitude to my advisor Prof. Weihua Jiang for the continuous support of my study and research since my master degree up to doctoral, for his patience, motivation, enthusiasm, and immense knowledge. His guidance helped me in all the time of research and writing of this thesis. I could not have imagined having a better advisor and mentor for my study.

I would like to thank Assistant Prof. Sugai for his technical support and insightful comments. I would also thank my doctoral dissertation committee, Prof. Harada, Prof. Sasaki, Prof. Kikuchi and Prof. Tokoi for their comments, advices and encouragements.

Thanks to staff of Extreme Energy-Density Research Institute for supporting and providing study facilities during my Master and Doctoral course. I thank all of my lab-mates actually my friends in Jiang laboratory for all technical and daily life support which I received. I always remember all the fun we have had in these years. Also thanks for Nagaoka University of Technology and its staff especially international affairs division who are always ready for supporting students in their daily life.

I wish to express my thankfulness from Japanese Government for providing me Monbukagakusho scholarship which is helping me to my dreams come true.

At the end I express my special and great appreciation to my wife for her amazing support and tolerance during these years and I would like to thank my family for supporting me spiritually throughout my life which helped me to get the place where I am now.

TABLE OF CONTENTS

Chapter Page

LIST OF FIGURES

LIST OF TABLES

1 CHAPTER I: INTRODUCTION

1.1 Background

1.1.1 Pulsed Power Technology

Pulsed Power is a certain amount of electrical energy released in a very short time. It has applications in many industrial and defense-related fields, owing to its unique characteristics in both power and time domains. Pulsed power is usually generated by the method of pulse compression where high power is achieved by compressing the time width of a required amount of energy. Over the last decades, various pulsed-power technologies have been developed for generating pulsed power of different energy and power levels. In the meantime, it has been realized that a high-power pulse can be obtained by synchronously releasing many lower power pulses to a common load. In other words, a required peak power can be obtained by adding up enough numbers of small pulses if they are synchronized. Linear transformer driver (LTD) is a pulsed-power generation scheme based on this concept [1].

1.1.1.1 Compressing energy and releasing it in a very short time

Pulsed power is the term used to describe the science and technology of accumulating energy over a relatively long period of time and releasing it very quickly, thus increasing the instantaneous power. Steady accumulation of energy, followed by its rapid release can result in the delivery of a larger amount of instantaneous power over a shorter period of time, although the total energy is the same. Energy is can be stored many different

ways. Electrostatic Fields (Capacitors), magnetic fields (Inductors), Mechanical Energy (through large flywheels connected to special purpose high current alternators), Chemical Energy (high-current lead-acid batteries, or explosives) (Fig. 1-1) [2].

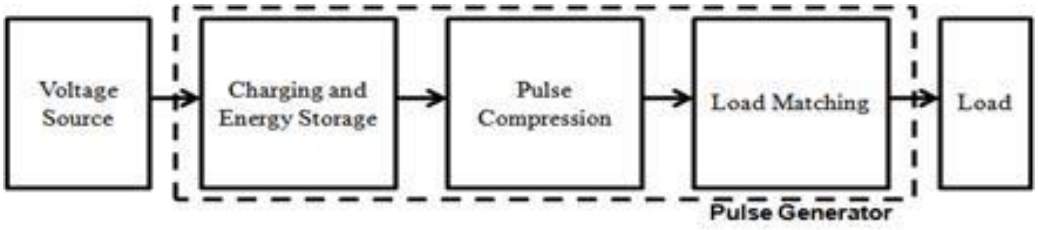

Fig. 1-1. Typical pulsed power system.

In following example the difference between releasing the energy in 1s and 1µs is shown. Releasing 1kJ energy in shorter time (1µs) provides peak power of 1GW (Fig. 1-2) [2].

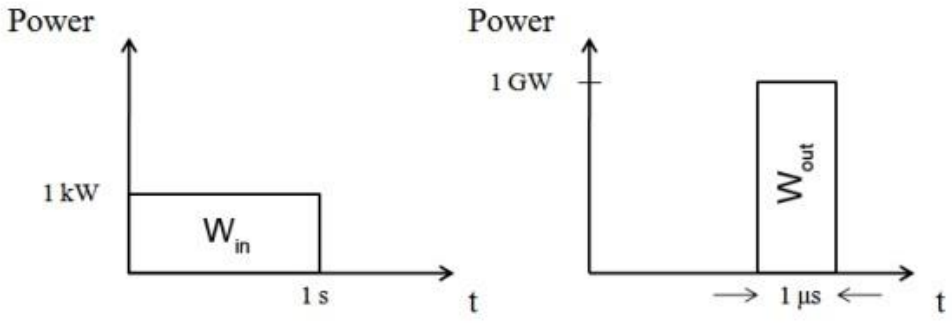

Fig. 1-2. Definition of pulsed power energy by example.

Pulsed power is usually generated by the method of pulse compression where high power is achieved by compressing the time width of a required amount of energy. Over the last decades, various pulsed-power technologies have been developed for generating pulsed power of different energy and power levels [2].

Historically, from very large pulsed power generators to desktop pulsed systems, the basic principle of pulse compression remained unchanged. Although these pulsed power sources have played important roles in experiments for scientific studies and industrial applications, their limitations have also been realized over the years. For example, the control of pulsed power compression process requires unavoidably switches that must be fast enough and powerful enough. The limitations of these switches usually set the upper limit of the output of a pulsed power system. In addition, the pulse compression method requires multiple energy storage components, which directly affects the system compactness. Furthermore, the pulse compression process offers very limited flexibility in the output waveform variation [3].

1.1.1.2 Synchronize energy and power adding

In the meantime, it has been realized that a high-power pulse can be obtained by synchronously releasing many lower power pulses to a common load. In other words, a required peak power can be obtained by adding up enough numbers of small pulses if they are synchronized. Linear transformer driver (LTD) is a pulsed-power generation scheme based on this concept [4].

Linear Transformer Driver (LTD) is a relatively new concept for pulsed-power generation. In the LTD scheme, the pulsed power is generated by a large number of

synchronized basic circuits, each consists of a capacitor (or capacitors) and a switch. The required Output power and output impedance of a system are obtained by connecting these basic circuits in parallel (for the current) and by adding their output inductively (for the voltage). Compared with traditional pulsed-power generation methods, LTD has the important features in stress breakup and modularity, which offer the possibility of building very large petawatt-class pulsed-power machines required by inertial fusion studies. On the other hand, compact repetitive pulsed-power technology has been under development for decades, aiming at industrial applications such as pollution control, laser pumping, and new type of particle accelerators. Here, power semiconductor devices are commonly used as the switches in order to achieve operation stability, compactness, and high repetition rate. However, these switches usually determine the system Output power and repetition rate. The reason is that the switching devices usually carry the heaviest burden of the whole system. From this point of view, the LTD features stated earlier, namely, stress breakup and modularity, are also very attractive to compact pulsed-power generation.Therefore, it looks meaningful to adapt the LTD concept to the needs of compact pulsed power. In this case, miniature LTD modules can be made of solid-state elements. In principle, arbitrary Output power and output impedance can be obtained by connecting necessary numbers of modules in parallel and in series, as in large LTD-based pulsed-power generators. The equivalent circuit of an LTD generator is shown in Fig. 1-3 each circuit unit consists of a capacitor and a switch. A certain number of such units are connected in parallel to form a module, and a certain number of such modules are added up inductively to form a stack. Furthermore, such stacks can be connected in different

ways so that, in principle, arbitrary output voltage and current can be realized by using appropriate combinations of units, modules, and stacks [4].

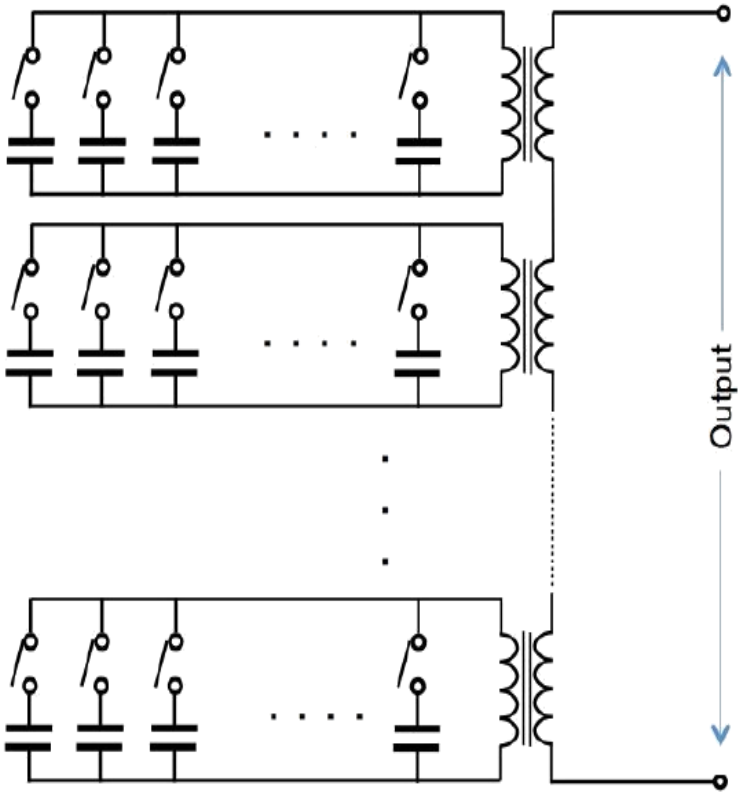

Fig. 1-3. Equivalent circuit of LTD generator

One of the potential applications that may require relatively precise waveform control is plasma generation by pulsed atmospheric discharge. It is known that pulsed gas discharge under atmospheric pressure is characterized by its time-varying impedance behavior. For this reason, a well-controlled time history of the applied voltage which is one of the greatest features of LTD may allow us to manipulate the discharge current during the process of pulsed atmospheric discharge [5].

1.1.2 Atmospheric Pressure Discharge

Atmospheric pressure discharge is an electrical discharge which is happening on the atmospheric pressure. An electrical discharge results from the creation of a conducting path between two points of different electrical potential in the medium in which the points are immersed. If the supply of electrical charge is continuous, the discharge is permanent, but otherwise it is temporary, and serves to equalize the potentials. Usually, the medium is a gas, often the atmosphere, and the potential difference is a large one, from a few hundred volts to millions of volts. If the two points are separated by a vacuum, there can be no discharge. The transfer of matter between the two points is necessary, since only matter can carry electric charge. This matter is usually electrons, each carrying a charge of 4.803×10^{-10} esu. Electrons are very light, 9.109×10^{-28} g, and so can be moved with little effort. However, ions can also carry charge, although they are more than 1836 times heavier, and sometimes are important carriers. Where both electrons and ions are available, however, the electrons carry the majority of the current. Ions can be positively or negatively charged, usually positively, and carry small multiples of the electronic charge. The two termini of a discharge are at different potentials. The higher, or positive, potential is at the anode, while the lower, or negative, potential is at the cathode. For a discharge to occur, there must usually be a source of electrons at the cathode, and the nature of this source controls the form of the discharge. Cosmic rays and natural radioactivity continually produce a small number of electrons and ions in all gases at the surface of the earth, and this gives air a small conductivity. The electrons will migrate to the anode, the ions to the cathode, and a small current will flow. This current has no visible effects, and can be detected and measured only with difficulty, but is

always present. Any charged body attracts charges of the opposite sign that sooner or later will neutralize its charge, though the usual reason for the loss of charge is conduction over the surface of the supports of the body, which is normally far greater than the small space current from the ions and electrons normally present in the air. More copious sources of electrons are necessary for a good discharge. One source is the photoelectric effect. Photons can also be absorbed by a molecule, which gives up an electron and becomes a positive ion. The photon energy hν must be greater than the energy required to free the electron, the *work function*. Electrons already in the discharge, such as the random electrons produced by cosmic rays and radioactivity, can add to their number by ionizing gas molecules by collision. Each ionizing collision produces a new electron, and a positive ion that moves the other way, an *ion pair*. An electron cannot do this unless it has acquired sufficient kinetic energy by being accelerated in an electric field. If an electron frees another by an ionizing collision, then these two can both free additional electrons, and so on. This creates an electron *avalanche*, which may send a burst of electrons toward the anode, leaving in their wake a cloud of slow positive ions that will make their way to the cathode. The net result is to multiply the original electron current, an effect used in gas phototubes to increase the photocurrent for a given amount of light. This does not start a sustained discharge, but merely increases the current that otherwise would be available. This type of discharge produces little light, so it is called a *dark* or *Townsend* discharge, after the man who studied them in detail first. Fig. 1-4 [6] shows electrical discharge in different regimes. That cloud of positive ions will sooner or later collide with the cathode. It is rather unlikely for a positive ion to snatch an electron from the few that are available while it is moving through the gas. Recombination is a

very difficult process, since only one particle is the outcome, rather than the three particles that come out of an ionization, so it is hard to conserve both momentum and energy [6] [7] [8].

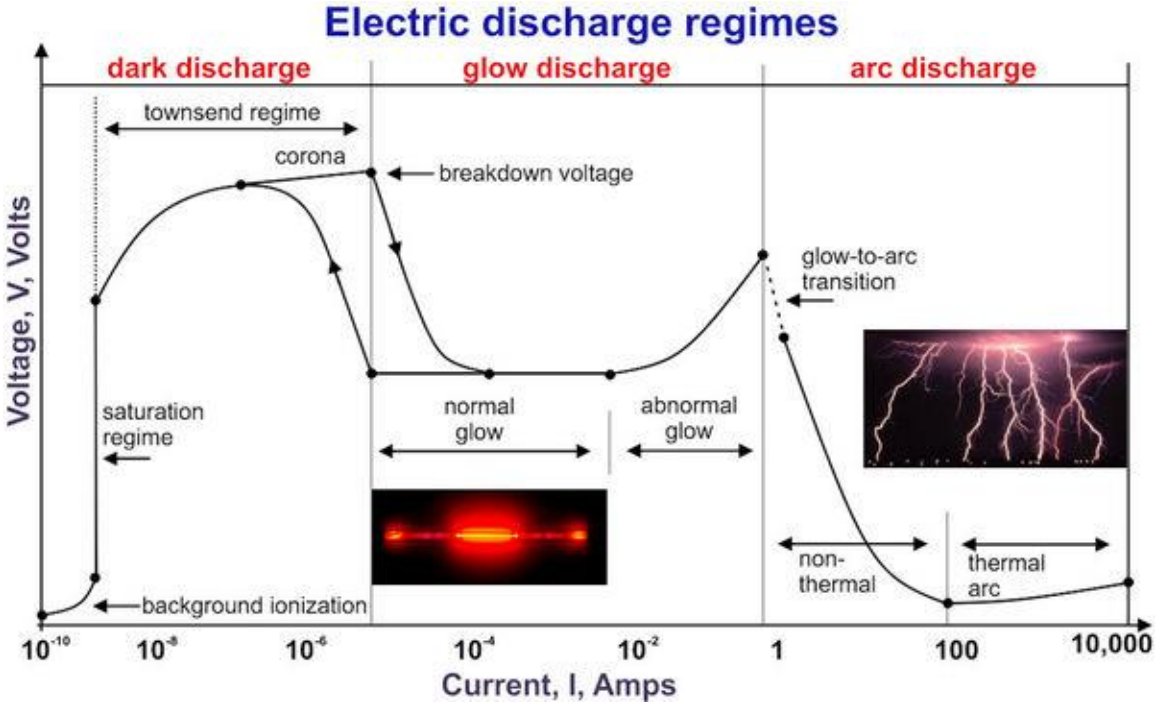

Fig. 1-4. Summary of Electric Discharge Regimes.

Therefore, most of the positive ions created in an electron avalanche reach a surface eventually, and they are driven to the cathode by the electric field. When they arrive, they recombine at the surface, and in some cases eject an electron. For Ne on an Fe cathode, one out of about every 45 ions produces an electron. However, if the electron avalanche produces more than 45 electrons, then there will be sufficient positive ions to replace the electron that originally left the cathode (or came in from elsewhere). Now the discharge produces its own electrons, without relying on cosmic rays or natural radioactivity, and

becomes *self-maintained*. This is a significant event in the life of a discharge, and usually means that the discharge becomes evident through light or noise. The potential between anode and cathode at which this occurs is called the *sparking potential* V_s. Now the whole path between anode and cathode becomes conducting because of the electrons and ions distributed along it. Unless something limits the current, such as the disappearance of the potential difference, it increases rapidly and without bounds. The ion bombardment heats up the cathode surface, which becomes incandescent, and begins to emit electrons thermionically, without reference to the number of ions coming in or the efficiency of the electron avalanche. Any spot that becomes hotter than its neighbor, tends to become even hotter as the extra thermionic electrons attract the positive ions to the spot. This, the final state of the discharge, is called an ***arc***. The name came from the way the path of the discharge, when arranged to be horizontal, rose in a flaming arch, or arc. It requires very little potential difference to support the arc, mainly just enough to keep the path of the discharge supplied with ions to replace those lost in various ways. A lightning stroke is an example of such a discharge, but with anode and cathode that are quite different from those in a carbon arc light. In the carbon arc light, the discharge is started by drawing the carbons apart, which produces an arc at once, since the discharge does not have the difficult task of establishing a conducting path over a great distance, as in lightning. An arc is also produced whenever an electric circuit is interrupted, and must be extinguished before it does any damage. The nature of a discharge depends, as we have seen, on the method for supplying electrons at the cathode, and on how the discharge is confined. The lightning stroke, and the carbon arc, are both unconfined arcs. The lightning stroke draws its electrons from the cloud, its cathode, and transmits them to the earth, its anode. The

carbon arc obtains its electrons from the cathode spot on the negative carbon, which it heats to incandescence. Both are self-confined, the surface of the conducting channel arranging itself so that the net outward current is zero. A discharge between metal electrodes in a glass tube that gets its electrons from positive-ion bombardment of the cathode, and is confined by the glass walls, is called a *glow discharge*. Glow discharges are useful and convenient to study, so their properties are very familiar, if not those of the majority of discharges. A discharge may exist in the vicinity of a sharp point, or other place with a small radius of curvature where the electric field is increased significantly from its average value. A negative potential on the point makes it a cathode, while the anode is an indefinite volume in the surrounding gas. A positive potential makes it an anode, and attracts electrons from an indefinite surrounding volume, which becomes the cathode. These two discharges look quite different with constant potentials, but with alternating current the opposites succeed one another and make an average impression. If the discharge occurs at about atmospheric pressure, it is called *corona*. In any discharge, multiple processes compete at the electrodes and in the gas, so explanations and theories can become subjects of dispute. Also, the variety of phenomena in discharges is very rich and depends on many factors, such as purity and surface preparation, which are difficult to quantify. The whole variety cannot be mentioned here, only what is typical under reasonable assumptions. There is great scope for thought and reasoning in this field, which makes it fascinating, along with the beauty of the phenomena [9] [10] [11] [12].

In addition, an electrical discharge is plasma, which is an ionized gas. Plasmas are sustained if there is a continuous source of energy to maintain the required degree of ionization and overcome the recombination events that lead to extinction of the discharge. Atmospheric discharges are thus difficult to maintain as they require a large amount of energy. In Table 1-1 [13] shows the characteristics of the various atmospheric plasma sources in terms of plasma properties (electron temperature and density, gas temperature) and working conditions (power supply, gas flow). The nature of the plasma gas is important since it influences the plasma temperature.

Table 1-1. Characteristics of atmospheric plasma sources

Excitation	Source	Plasma properties	Operating conditions
Industrialized sources			
DC/Low frequency	Arc torch	$T_e = T_h \approx$ 8000–14,000 K[s]	Gas. Ar /He
		$n_e = 10^{21}$–10^{26} m^{-3}	Gas flow. 10–150 slm
			Power. 10–100 kW
	Plasmatreat	T_h < 700 K	Gas. air
			Gas flow. 117 slm
Pulsed DC/Low frequency	Corona	T_e = 40,000–60,000 K	Gas. air
		T_h < 400 K	
		$n_e = 10^{15}$–10^{19} m^{-3}	
	DBD	T_e = 10,000–100,000 K[m]	Some 100 W
		T_h < 700 K	Plasma gas. 5–40 slm
		$n_e \approx 10^{18}$–10^{21} m^{-3}	
Radio frequency	ICP	$T_e = T_h$ = 6000–11,000 K[s]	Gas. Ar/He
		$n_e = 10^{21}$–10^{26} m^{-3}	Gas flow. 10–200 slm
			Power. 50–700 kW
Pulsed radio frequency	IST	T_h < 400 K	Gas. surrounding air
			No gas flow
			Power. 20 kW
Microwave	Cyrannus	T_h < 700K	Gas. Ar/O_2
			Power. 6 kW
Still in laboratory development sources			
DC	Microplasma	–	Power. 500 V; 250 μA
Radio frequency	APPJ	T_e = 10,000–20,000 K[s, m, l]	Gas. O_2 /He
		T_h < 600 K	Gas flow. 50–90 slm
		$n_e = 10^{17}$–10^{18} m^{-3}	Power. some 100 W
	Cold plasma torch	T_e = 10,000–20,000 K[s, l]	Gas. Ar
		T_h < 700 K	Gas flow < 1 slm
		$n_e = 10^{17}$–10^{18} m^{-3}	Power. 100 W
	Hollow cathode	T_e = 3000–11,000 K[s]	Gas. Ar, He
		T_h < 800 K	Gas flow < 2 slm
		$n_e \approx 10^{17}$–10^{18} m^{-3}	Power. some 100 W
	Microplasma CCμP	T_e = 1850–2300 K	Gas. Ar
			Gas flow. < 0.2 slm

Excitation	Source	Plasma properties	Operating conditions
			Power. 5–25 W
Microwave	TIA	T_e = 13,000–14,000 K [s]	Gas. He
		T_h = 2400–2900 K[s]	Gas flow. 2–6 slm
		$n_e \approx 10^{21}$ m^{-3}	Power. 100 W–2 kW
	MTD	T_e = 17,000–20,000 K[s]	Gas. N_2
		T_h = 1500–4000 K[s]	Gas flow. 1–3 slm
		$n_e = 10^{20}$–10^{21} m^{-3}	Power. 100 W–400 W
	MPJ	T_e = 12,000–17,000 K[s]	Gas. Ar
		T_h = 5000–10,000 K[s]	Gas flow. 2–7 slm
		$n_e \approx 10^{22}$ m^{-3}	Power. 2–5 kW
	MPT	T_e = 16,000–18,000 K[s]	Gas. Ar
		T_h = 3000–3500 K[s]	Gas flow < 1 slm
		$n_e = 10^{20}$–10^{21} m^{-3}	Power. some 100 W
	Baeva et al.	$T_e \approx$ 7000 K[s]	Resonant cavity
		$T_h \approx$ 7000 K[s]	Pulsed MW power supply
		$n_e \approx 10^{19}$ m^{-3}	Gas. N_2
			Gas flow. 30 slm
			Power. 800 W
	Sugiyama et al.	$T_e \approx$ 90,000 K[s]	Ignition by perovskite powder
		$T_h \approx$ 1000 K[t]	Gas. Ar/H_2
		$n_e \approx 10^{17}$ m^{-3}	Gas flow. 0.3–1.2 slm
			Power. some 100 W

1.1.2.1 Applications of the various atmospheric plasma sources

Atmospheric pressure plasma is capable of treating many different surface types and materials such as plastic, metals, glass, ceramic and hybrid materials. Since they do not require chambers, it is much easier to incorporate atmospheric pressure plasma machines into automated industrial manufacturing lines. This is a vital capability since plasma technology is becoming more widely used in many industries. Unfortunately, these atmospheric pressure plasma treatments are limited to 2-dimensinal surfaces whereas low-pressure plasma systems are capable of treating 3-dimensional objects of most shapes. Atmospheric pressure plasma can also be used in the small scale. Devices called plasma pens are atmospheric pressure plasma systems that are handheld and capable of very detailed surface activation and cleaning. There are different kinds of applications for atmospheric plasma as Spectroscopic analysis, Gas treatments (Cleaning, Synthesis), Material processing (Surfaces treatments, Surface cleaning, Surface etching, Surface activation, Bulk material treatments, Powder treatment, Toxic wastes treatment, Material machining, Metallurgy, Lamps, etc…[13].

1.1.3 Pulsed Corona Discharge

In this study, the electrode of atmospheric discharge load arrangement has a typical corona discharge configuration. The corona discharge plasma is being generated between two electrodes by applying high voltage pulses in atmospheric pressure. Pulsed corona discharge as one of the efficient type of atmospheric pressure plasma sources has many different industrial application.

Corona discharges are relatively low power electrical dis- charges that take place at or near atmospheric pressure. The corona is invariably generated by strong electric fields associ- ated with small diameter wires, needles, or sharp edges on an electrode. Corona takes its name ("crown") from mariner's observation of discharges from their ships' masts during electrical storms. The corona appears as a faint filamentary discharge radiating outward from the discharge electrode. Because the corona is relatively easy to establish, it has had wide application in a variety of processes. Corona process applications emphasize one of two aspects of the discharge. The ions produced or the energetic electrons producing the plasma. The ion identities depend on the polarity of the discharge and the characteristics of the gas mixture, specifically on the electron attaching species. The electron energies depend on the gas characteristics and on the method of generating the corona. In general, in an application using ions, the corona induced plasma zone will occupy a small fraction of the total process volume, while a process using the electrons will fill most of the volume with the plasma [14] [15].

1.1.3.1 Type of Corona Discharge

Corona discharges exist in several forms, depending on the polarity of the field and the electrode geometrical con- figurations. For positive corona in the needle-plate electrode configuration, discharges start with burst pulse corona and proceed to the streamer corona, glow corona, and spark dis- charge as the applied voltage increases. For negative corona in the same geometry, the initial form will be the Trichel pulse corona, followed by pulseless corona and spark discharge as the applied voltage increases. For a wire-pipe or wire-plate electrode configuration, corona generated at a positive wire electrode may appear as a tight sheath around the electrode or as a streamer moving away from the electrode. Corona generated at negative electrodes may take the form of a general, rapidly moving glow or it may be concentrated into small active spots called "tufts" or "beads." Negative corona generally propagates by impact ionization of the gas molecules. Positive corona depends more on photoionization for its propagation. The positive streamer, for example, may advance at as much as one percent of the speed of light. In either case, the ultraviolet photon flux from ion-electron recombination is quite large. The positive sheath form is known as a Hermstein's glow and is similar to the discharge (at lower pressures) in a Geiger tube. It is characterized by a steady current at a fixed voltage, quiet operation, and almost no sparking. The positive streamer corona is a discharge confined to a narrow channel which originates at the electrode. It produces an unsteady current (because the streamer is repetitive), is quite noisy, and is the direct precursor to a spark. Once streamers form at an electrode, the sparking potential has almost been reached. The negative glow usually requires clean, smooth electrodes to form. The glow is made up of individual electron avalanches which trigger successive

avalanches at nearby locations. The total current from the electrode is relatively steady, but it is composed of many tiny pulses. The discharge is noisy and the sparking potential is high compared with the positive streamer corona. The glow often changes with time into the tuft form, a process associated with the formation of more efficient mechanisms of generating successive avalanches. The tuft corona is also noisy and has a similar sparking potential to the glow form. The average current is steady, but is composed of tiny pulses like the glow corona. The tuft corona is more spatially inhomogeneous than the glow corona. Differences between negative tuft and glow coronas have been investigated recently. The corona discharge is usually space-charge limited in magnitude, since the plasma emits ions of one polarity that accumulate in the inter electrode space. This gives the corona a positive resistance characteristic. Increases in current require higher voltages to drive them. If the current in the discharge is raised sufficiently, additional current-carrying species will be produced and spark discharges will result. The spark is usually characterized by a negative resistance characteristic, but the transition from corona discharge to spark discharge is not sharply defined [15].

Pulsed corona discharges can be applied in the form of discrete pulses, typically with lengths in the order of ns to microseconds. Because a pulsed discharge can operate at much higher peak voltages and peak currents for the same average power as in a d.c. glow discharge, higher instantaneous sputtering, ionization and excitation can be expected, and hence better efficiencies (e.g. better sensitivities for analytical spectrochemistry). This is because the basic plasma phenomena, such as excitation and ionization, are highly non-linearly dependent on field strength [16].

For the same reason, also in the semiconductor industry, pulsed power operation has emerged as a promising technique for reducing charge-induced damage and etches profile distortion, which is associated with continuous discharges. Another advantage of pulsed technology glow discharges compared to radio frequency technology is the simpler method of up-scaling due to reduced impedance matching network and electromagnetic interference problems, and the lower price of power supplies for larger reactors.

As far as basic plasma processes are concerned, a pulsed discharge is very similar to a d.c. discharge. It can be considered as a short d.c. discharge, followed by a generally longer afterglow, in which the discharge burns out before the next pulse starts. It should be mentioned that non-LTE is facilitated in pulsed discharges, because there is no excessive heating so that the gas temperature is lower than the electron temperature. Moreover, there is also non-chemical equilibrium because ionization (fragmentation) occurs on a different time-scale compared to recombination (on vs. off period) [17].

1.2 Diagnostics

1.2.1 FPGA as LTD Control Signal Source

In the first part of this study, we have tried to develop control system of Linear Transformer Driver (LTD) for its best performance. The used LTD is a compact pulsed power generator based on modularity performance. These modules can be controlled individually, in groups or all in a same manner. Based on load characteristic and desired output, proper control signals need to be delivered to the modules. The first challenge was to find a proper, compact control signal source for LTD. This source should be flexible, fast, and compact with ability of producing multiple outputs for different

numbers of modules. We have found FPGA device as a perfect match for this kind of usage. We developed the hardware of system and developed the FPGA program to be matched with our needs.

1.2.2 Pulsed Atmospheric Discharge

There are two main issues which are being addressed, explored and explained by experiments and designed model. Also new method is included to solve the problem in 1st case. The problems are:

- Significant current increase in discharge process in case of applying longer voltage pulse.
- Current leakage in repetitive operation of pulsed atmospheric discharge

1.2.2.1 Instable plasma and time-varying impedance of atmospheric discharges

Non-equilibrium plasma has some advantages over thermal equilibrium. It is easier to apply electromagnetic fields than to uniformly heat and confine plasma. However, electromagnetic fields naturally transport charged species whose concentrations and energies therefore naturally vary in space, particularly, close to the walls of the container. Generically, the species in such a plasma are not in thermal equilibrium. And it is energy efficient to not feed energy equally into all degrees of freedom within a gas or plasma, such as into the thermal displacement, rotation, and vibration of neutral molecules, but only into those degrees of freedom that can efficiently create the desired final reaction products for the particular application. Therefore it is frequently preferable to accelerate only electrons to high velocities and let them excite and ionize molecules by impact while

keeping the gas cold. If the electron energy distribution is appropriate, some reactions can be triggered very specifically [18]. Non-equilibrium plasmas are characterized by charged species with a much higher kinetic energy than neutral species [19].

This is why study and explorer of plasma behavior in this case is more complicated than the thermal equilibrium plasma. The pulsed atmospheric discharge is known for its time-varying impedance where constant voltage usually does not result in constant current. High electric field is causing rapid development of plasma near to the main electrode when longer voltage pulses are being applied. There are some investigation on boundary layer control [20] or impedance calculation and matching [21] but researches on plasma generation and its current control method in pulsed atmospheric discharge using pulsed power generators are rare and hard to find. This research is going to investigate this problem and offer a solution by using Solid-State Linear Transformer Driver (LTD) and Field Programmable Gate Array (FPGA).

1.2.2.2 Current leakage in repetitive operation of pulsed atmospheric discharge

The other phenomenon which has been explored in this study is about consecutive operation of pulsed atmospheric discharge. Repetitive operation of atmospheric pressure discharge has a significant role on system efficiency [22] and it is needed for many applications [23] therefore study and explore the phenomena is highly desirable research. This research has done an investigation with its own method on the mentioned issue. During the experiment the space charge effect has been observed on the following pulses as leakage current in a consecutive operation.

In a pulsed corona discharge the wire electrode (anode) is positive (positive corona), so the newly created negative charges are strongly attracted and falls to the wire electrode and produce by impacts destructive effects, the positive charges are on their side repelled toward the pipe electrode. They create a sort of positive cloud in the region immediately outside the glow which is on its side quasi neutral (ionization area). The electric cloud creates a field which is turned in its left side toward the anode and in its right side toward the cathode. The effect of the cloud is to reduce the field in the wire side and this is why it can be called the screening effect (Fig. 1-5) [24].

This topic has been discussed in some researches [25] [26] but in this research to explorer this positive charges effects we have designed a model which allow us to calculate the electric filed in two states, without positive residual charge and with positive residual charge. Finally, it has provided a physical interpretation of this effect from a different perspective.

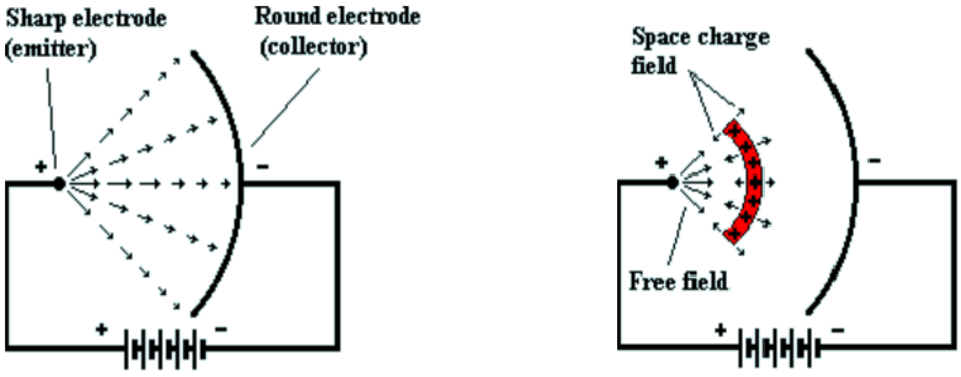

Fig. 1-5. (a) State without positive residual charges. (b) State with residual charge (screening effect).

1.3 Research Objectives

We have developed a relatively new type of pulsed voltage generator by using a circuit scheme called linear transformer driver (LTD). This research is going to show that for a solid-state LTD system, different modules can be switched at different timings so that the output voltage waveform can be shaped by adding together the individual output of all modules. This feature offers the possibility of arbitrary waveform composition through proper control of each LTD module without changing any hardware of the system. An ideal device for carrying out such kind of multichannel timing control is the field-programmable gate array (FPGA) which, if properly programmed, can provide enough number of independent signals timed with the internal clock.

One of the potential applications that may require relatively precise waveform control is plasma generation by pulsed atmospheric discharge. It is known that pulsed gas discharge under atmospheric pressure is characterized by its time-varying impedance behavior. The motion of the electrons near the ionization front is shown to be responsible for the propagation of the ionization front.

Also it has been investigated that the properties of the discharge plasma depend strongly on the characteristics of the input voltage pulses, i.e., voltage strength, pulse width and rise time. It is also shown that the stationary corona discharge without accompanying arc breakdown can be created by appropriately selecting the voltage pulse parameters for a given reactor geometry [27].

Therefore waveform control of this kind of application is very important. This paper reports a delicate experiment where LTD is operated by using a FPGA so that its output

voltage waveform can be adjusted in an arbitrary manner. As a result, the current waveform obtained on the discharge load can be controlled precisely to meet the requirement of the applications. This kind of the waveform control is expected to have significant impact on the industrial applications of atmospheric discharge. The experimental system and results are shown by details in this part of study.

Also we have tested the LTD-type pulsed voltage generator with a pair of coaxially configured electrodes and demonstrated load impedance control by carrying out voltage waveform control. In this part of research, we have used our LTD-type pulsed voltage generator to study the influence of a pulsed atmospheric discharge on the behavior of the following pulse for consecutive operation. Since applications of pulsed atmospheric discharge require repetitive operation, it is always important to know and to understand the effect a pulsed discharge can create in the gas that may result in different behavior of the next pulse following it. This research is going to prepare a physical interpretation on this topic by its designed model.

2 CHAPTER II: LINEAR TRANSFORMER DRIVER (LTD)

2.1 LTD Concept

2.1.1 Power Adding

The linear transformer driver (LTD) method of pulsed power generation is a different approach from that of pulse compression. By adding up a large number of low-power pulses, one can obtain a relatively high-power pulse, as shown in Fig. 2-1 In this case, since no switch is required to handle the total Output power, there is no fundamental limit on the Output power of the system. An LTD-based pulsed power system is usually more compact compared with a pulse compression system of the same output level because it does not require intermediate energy storage components. However, to achieve best power adding, the timing of all small pulses must be perfectly synchronized.

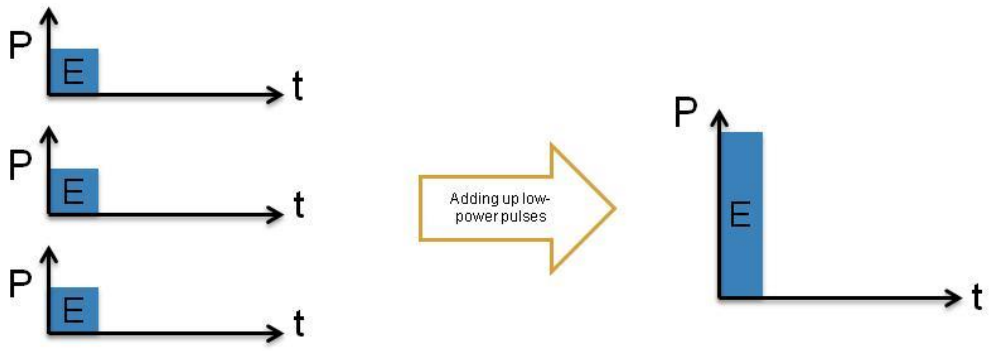

Fig. 2-1. Power adding concept.

2.1.2 Power Shaping

The concept of power adding of LTD can be further extended to that of pulse shaping. By adding small pulses to each other with adequate relative timing, one can obtain a desired output waveform, as shown in Fig. 2-2. In other words, by intentionally desynchronizing the small pulses of LTD with adequate timing control, we can shape a pulse using small pieces. The capability of pulse shaping enables flexible variation of output waveform and optimization of generator performance.

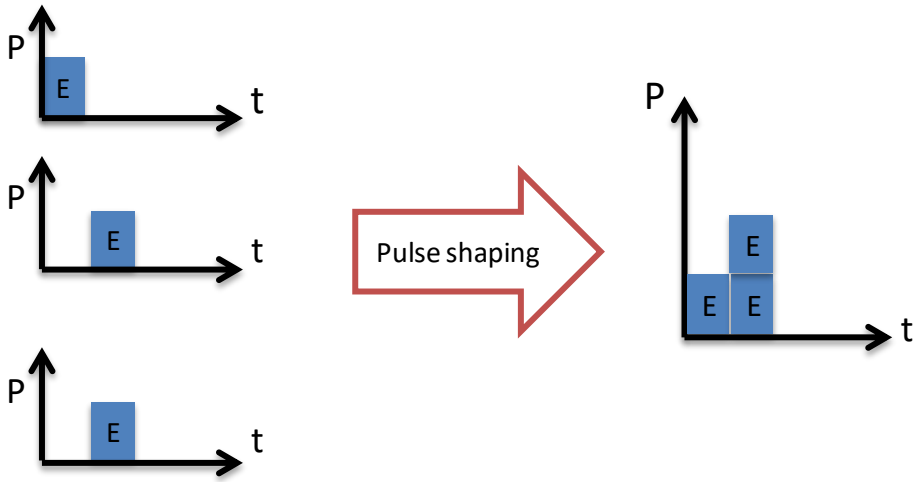

Fig. 2-2. Pulse shaping concept.

2.2 LTD Circuit, Structure and Principal

Compared with a traditional pulse-compression scheme, pulsed-power generation by LTD has advantages in the following respects.

1) There is virtually no physical limit on the output parameters of a system.

2) An LTD-based pulsed-power system can be constructed by using premanufactured modules.

3) It allows controlled time variation of output voltage, current, and source impedance during the pulse.

Large LTDs using spark gap switches have been studied for many years, aiming at potential applications to inertial fusion drivers. On the other hand, compact LTDs based on solid-state switches are also under development for industrial purposes. Compared with large LTDs, solid-state LTDs have advantages in high repetition rate and switching OFF capability. A series of studies has been carried out to demonstrate the uniqueness and usefulness of solid-state LTD. An LTD module using 24 metal–oxide–semiconductor field-effect transistors (MOSFETs) has been developed to study the essential behavior of the module. In this paper, an LTD stack consisting of 30 modules has been developed and used to study both power adding and pulse shaping.

2.2.1 MOSFET-Based LTD Module

The front-view photograph of the solid-state LTD module is shown in Fig. 2-3 and its main components are listed in Table 2-1.

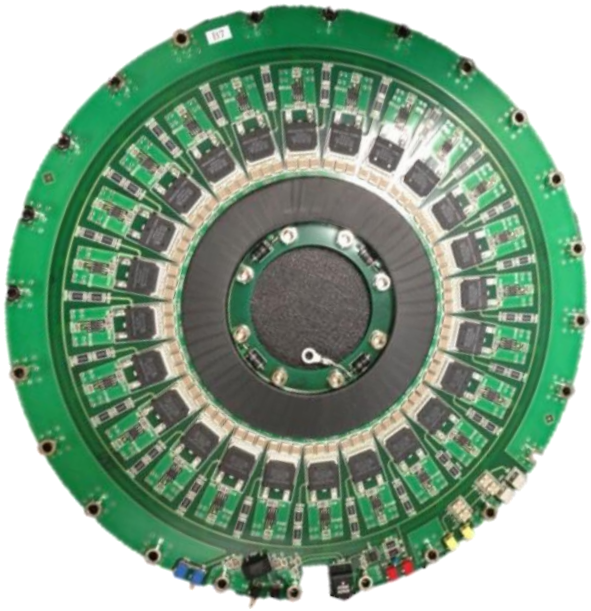

Fig. 2-3. LTD module front-view

Table 2-1. Major devices in each Module

Device	Manufacturer	Model	Specifications	Number per module
MOSFET	IXYS	IXFT6N100F	1000V,6A(DC)	24
Driver IC	MIcrochip	MCP1407	4.5~18V,6A	25
Capacitor	Murata	GRM55DR73A	1kV,100nF	72
Magnetic Core	Sichuan Liyuan Electronics	1K107	$130mm^{f}$(OD) × $5mm^{t}$	1
Optic receiver	HITACHI	DR9300	DC~50Mb/s	1
Diode	Semikron	SKA3/17	1700V,3A(DC)	4

The equivalent circuit of the LTD module is shown in Fig. 2-4. The operation principle of the module is summarized as follows. The control signal is delivered to the module through an optic fiber. It is received by an optic receiver and amplified by a driver integrated circuit (IC) before being sent in parallel to all 24 driver ICs of the MOSFETs. The 24 MOSFETs are switched simultaneously generating pulsed output voltage between the top and bottom electrodes on the inner side of the circular module. The magnetic core prevents significant current leakage through the case of the module. Therefore, when many modules are stacked together, the output voltages generated by all modules are added up as the system output between the top electrode of the highest module and the bottom electrode of the lowest module. Protection diodes are connected between the output electrodes, as observed in Fig. 2-4. These diodes play an important role in protecting the module from external reverse voltage. It is important to note that these diodes can effectively bypass the circuit current driven by other modules when the local MOSFETs are not switched ON, allowing different switching timings of different modules.

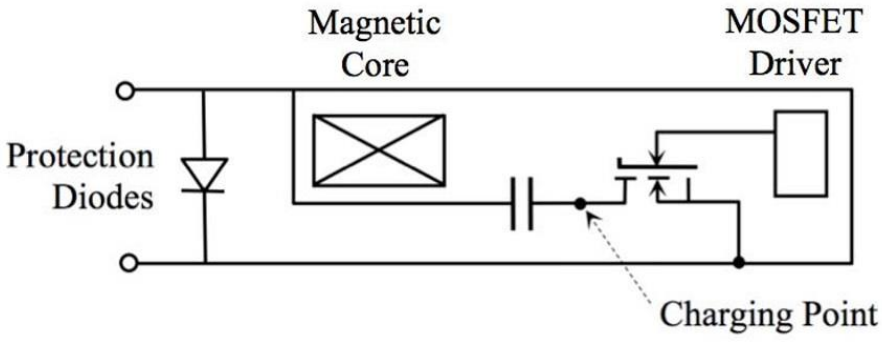

Fig. 2-4. Equivalent of LTD module circuit.

2.2.2 Pulse Generator as a Control Signal Source of LTD

LTD concept is based on pierces synchronization of pulses which is highly desirable by using fast, compact and flexible control signals. Therefore the control signal source is very important device on this stage.

MOSFET gate circuit is shown in Fig. 2-5 which in this case, control signals are provided by a pulse generator. As it was told before, one of the most significant advantages of LTD is pulse shaping which can be obtained by using different numbers of modules with different synchronization time. Pulse generators are very limited in this case because of their limited output channels. Also they are heavy and outputs are limited by manual inputs.

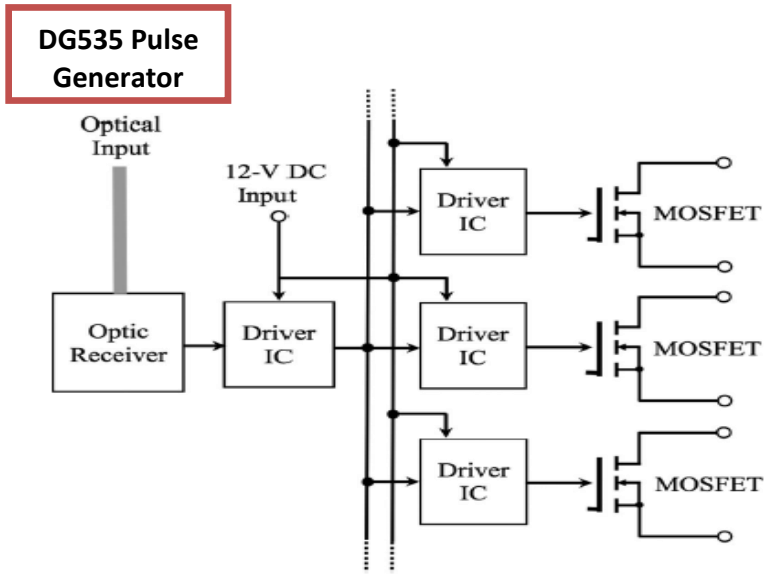

Fig. 2-5. Circuit diagram for MOSFET gate control on each module

In Fig. 2-6 [4] time relation between signals in LTD is shown when a pulse generator is used for control signal source. Upper waveform is signal control waveform.

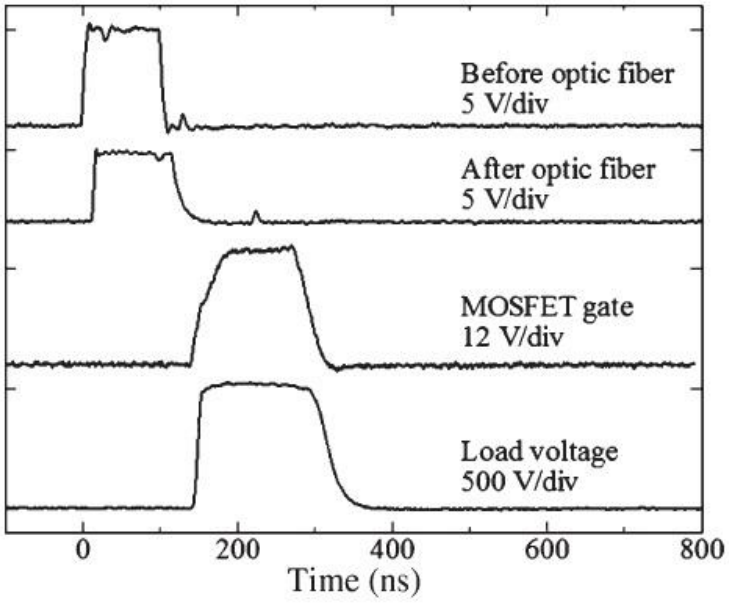

Fig. 2-6. Time relation between signals in LTD

2.2.3 Field Programmable Gate Array (FPGA) as Control Signal Source of LTD

In the other side, the **field-programmable gate array (FPGA)** is a semiconductor device that can be programmed after manufacturing. Instead of being restricted to any predetermined hardware function, an FPGA allows you to program product features and functions, adapt to new standards, and reconfigure hardware for specific applications even after the product has been installed in the field—hence the name "field-programmable". User can use an FPGA to implement any logical function that an application-specific integrated circuit (ASIC) could perform, but the ability to update the functionality after shipping offers advantages for many applications [28]. Multiple I/O pins, clock speed variation and functionality are significant specifications of FPGAs.

Fig. 2-7, shows a simple comparison between specifications of pulse generator and FPGA as signal sources for LTD.

The LTD stack consisting 30 modules. Those modules can be controlled as one group, groups or individually based on the application request. Therefore in each case different type of control signals are needed.

For example if modules outputs are needed individually, each module should run with their own dedicated control signals. It means 30 different control signals for 30 modules are needed. In these case multiple IN/OUT pins of FPGA are very useful. Also the

programmability of FPGA helps us to change the control signals specification based on the output request, easily and quickly.

In Fig. 2-8, control signals from FPGA's I/O pins are being delivered to the main driver IC by optic fibers. After the amplifying, these control transfer to the MOSFET's gate through a driver IC.

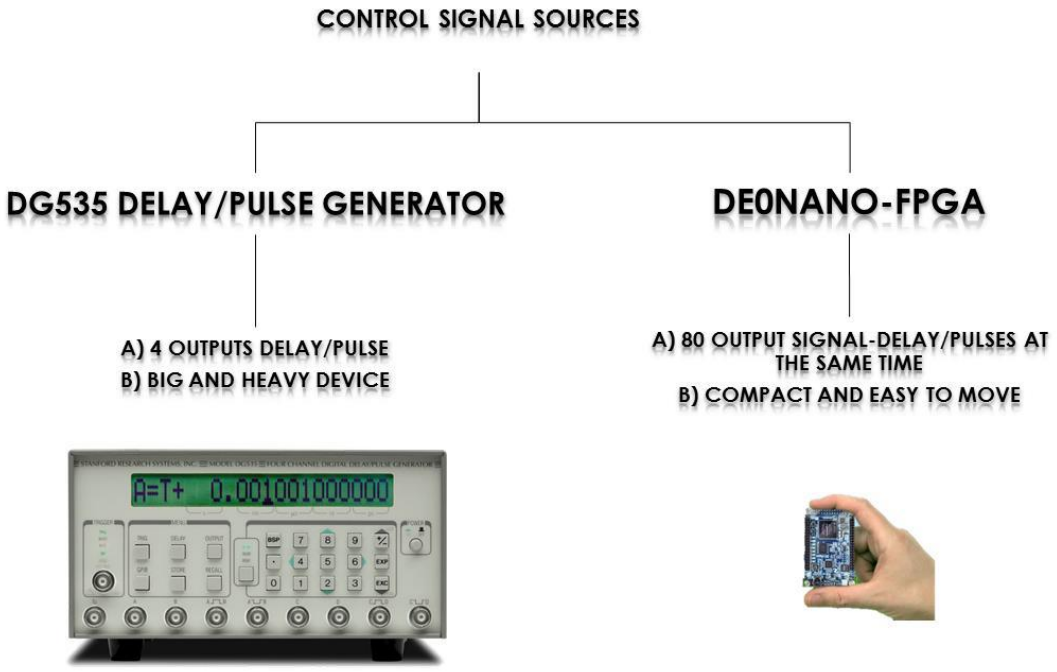

Fig. 2-7. Comparing of FPGA with Pulse Generator for LTD control.

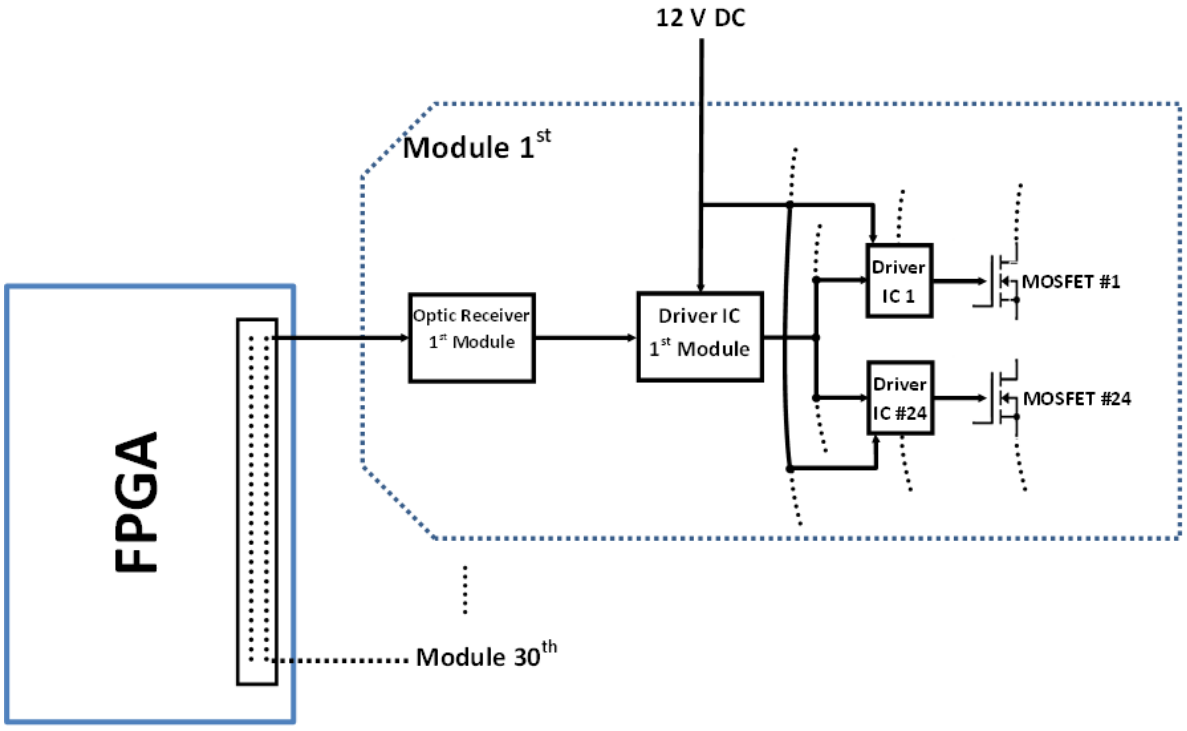

Fig. 2-8. FPGA I/O pins with its connection to gate circuit of MOSFETs.

2.2.3.1 DEO-Nano Cyclone IV FPGA

DE0-Nano is used FPGA for this study. Its top view and block diagram are shown in Fig. 2-9 and Fig. 2-10 [29] respectively. There are many parts in this FPGA for many different usage purposes but the main components that are important to us are.

- **Three 50MHz clock sources from the clock generator**
- **Two 40- I/O pin expansion header with diode protection**
- **5 fractional PLLs**

With using 50 MHz FPGA clock we can provide control signals with pulse width of 20 ns but with using PLL function we could increase the clock speed up to 200 MHz. In this case the provided control signals widths are 5 ns.

Also using the two 40 I/O pins header can give us 80 output pins which in our study we only need 30 of them.

Fig. 2-9. DE0-Nano top view.

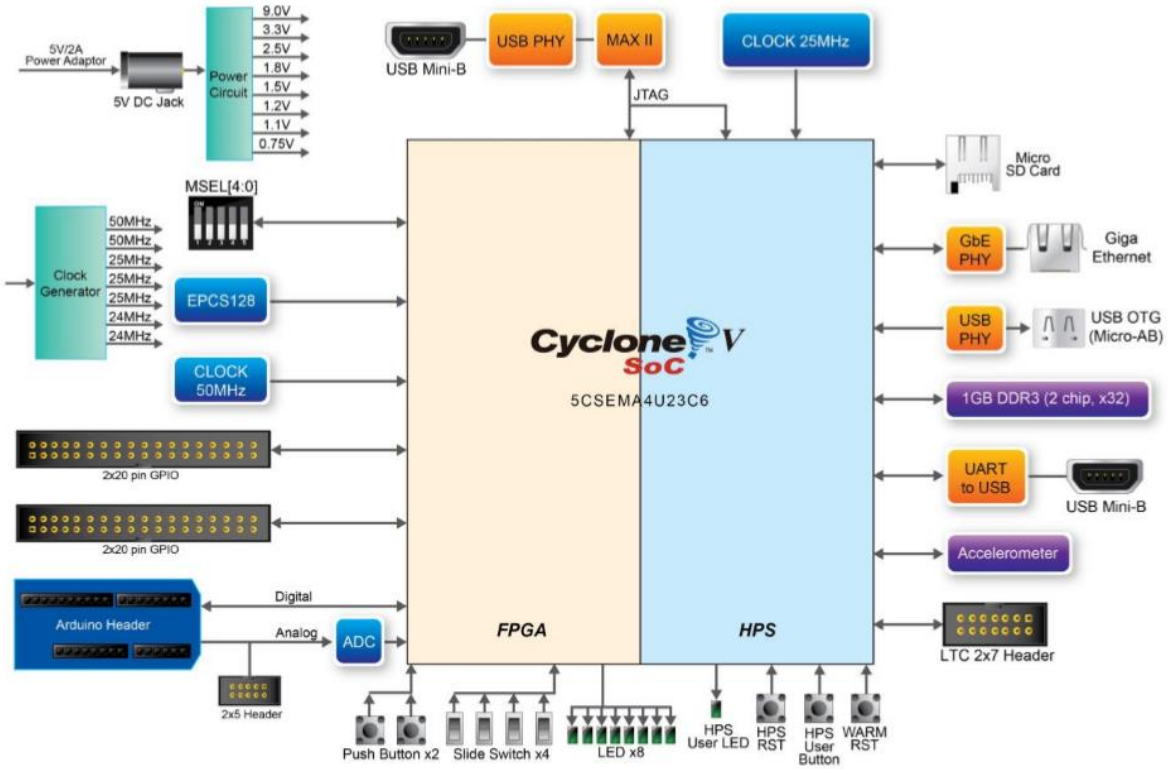

Fig. 2-10. DE0-Nano block diagram

3 CHAPTER III: LTD AND FPGA COMBINED SYSTEM

3.1 LTD Performance with Using FPGA Control Signals

Thirty LTD modules are stacked together, as shown in Fig. 3-1 [5]. A conducting sheet on the inner surface of a polyester pipe (5 mm in thickness) located at the center is connected with the bottom electrode of the lowest module. This conducting sheet works as a center conductor bringing the bottom potential to the top so that the output voltage of the stack is applied on the load resistors connected between it and the top electrode of the highest module.

Fig. 3-1. LTD stack with 30 modules.

The LTD stack has a diameter of ~30 cm and a height of~35 cm excluding the load resistors. It weighs about 23 kg. A continuous dc of 2 A is used for magnetic flux restoration through a wire winding of two turns around the whole stack. Very large blocking inductors are used to isolate the current source from the winding. The output of the LTD stack is diagnosed by measuring the output voltage across the load resistors using a high-voltage probe (PHV 4002). A digital oscilloscope (Tektronix TDS7104) is used for data recording. Fig. 3-2 [4] shows the waveforms of output voltage obtained with different charging voltages. It is seen that, as the charging voltage is increased from 100 V to 1 kV, the peak output voltage increases from ~3 to~29 kV, confirming the voltage multiplication by inductive voltage adding.

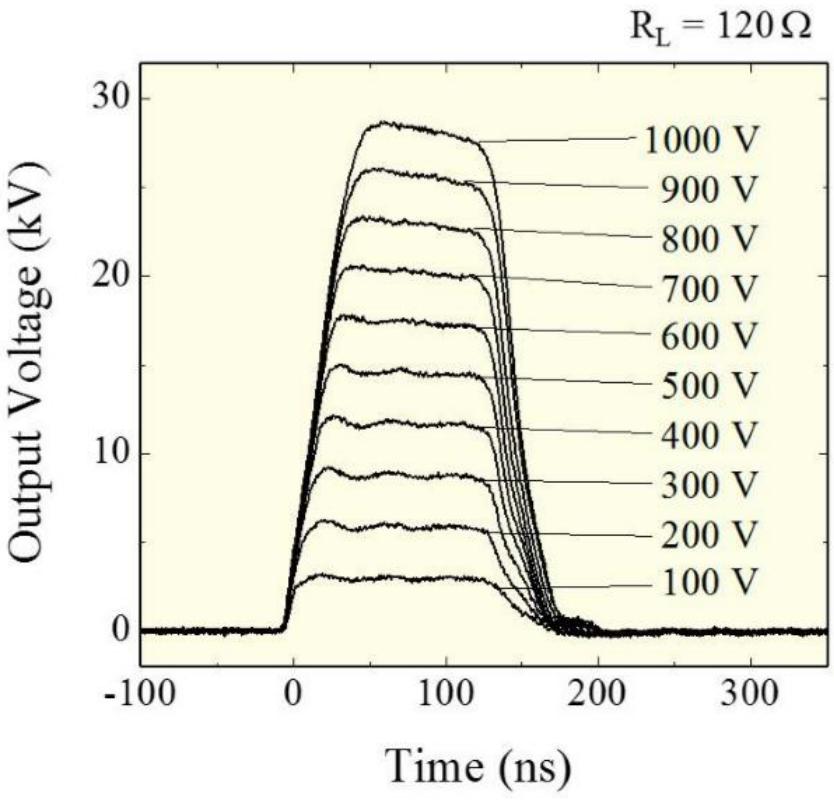

Fig. 3-2. Typical waveforms of the output voltage, obtained with different charging voltages.

Our LTD stack is capable of generating pulsed voltage up to 30 kV with maximum current of 300 A and pulse length variable in the range of 60~200 ns. It is noted that the output is ended by switching-OFF of the MOSFETs and the capacitors are far from complete discharge after one pulse. In this case, the circuit inductance has minor effects and the output voltage nearly equals that of the capacitors.

Fig. 3-3 [5], shows the waveforms of output voltage obtained with different pulse length of the control signal, when all 30 signals are synchronized. As the pulse length of the control signal is increased from 60 to 200 ns, the full width at half-maximum of the output-voltage pulse increased from ∼50 to ∼170 ns, indicating that the output pulse width can be continuously varied by changing the pulse length of the control signal. However, this pulse width variation is apparently limited within a certain range by two factors. On the shorter end, it is limited by the rise time of the system and, on the longer end, it is limited by the saturation of the magnetic cores. For example, for the case of 60 ns, the output is switched OFF before reaching its maximum. On the other hand, for the case of 200ns, the output pulse length is not sufficiently longer than that of 180 ns, indicating possible core saturation. Therefore, in principle, the shorter limit can be reduced by improving the switching performance and the longer limit can be raised by decreasing the operation voltage per module or by increasing the size of the magnetic cores. Finally, it should be added that the capacitance is large enough so that it does not have any effects on the pulse width except for a slight voltage droop during the pulse.

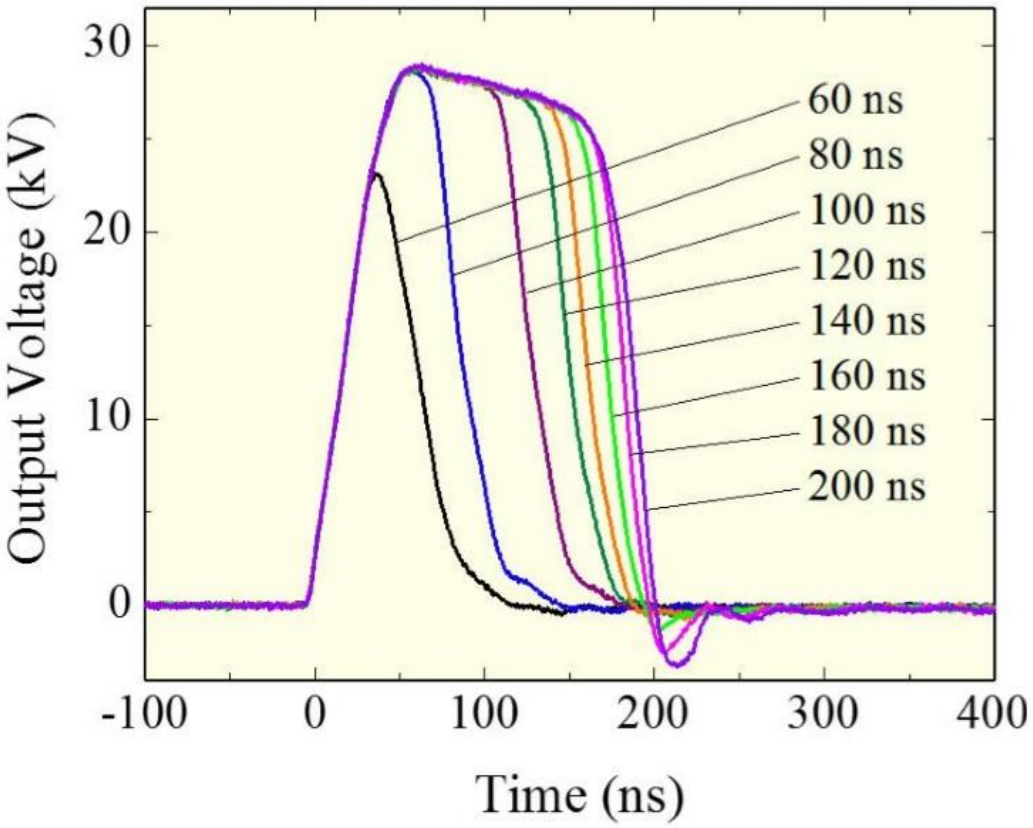

Fig. 3-3. LTD output voltage obtained by different pulse length of control signal.

3.1.1 30 Modules with Control Signals with Same Timing

The control signals are generated using a FPGA board (Altera Cyclone IV), which has 80 output pins. In this experiment, 30 of these output pins are used to control our 30 LTD modules individually. Each pin is linked with one of the modules through an optic fiber. By properly programming the FPGA board, we can send ON/OFF command to each module at any timing defined by the internal clock of 50 MHz. In this experiment all modules receive control signals with same timing specification (same ON and OFF timing). In Fig. 3-4 this process is illustrated. By prices synchronization, power adding is done for all 30 modules energy.

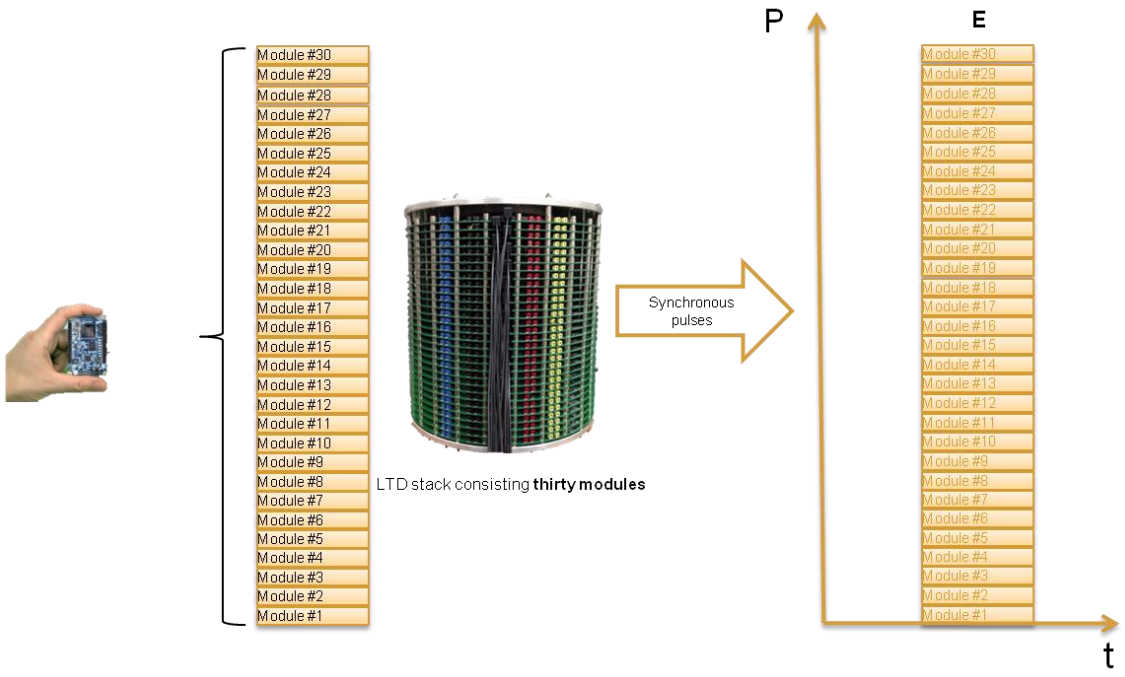

Fig. 3-4. LTD output energy illustration when modules are switched in a same timing manner.

In Fig. 3-5, LTD output when modules are switched with control signals with same timing is shown.

LTD input parameters: Charging voltage 1 [kV], Input current 74 [mA], Frequency 100 [Hz], Pulse width 80 [ns], Resistance 117.5 [Ω]

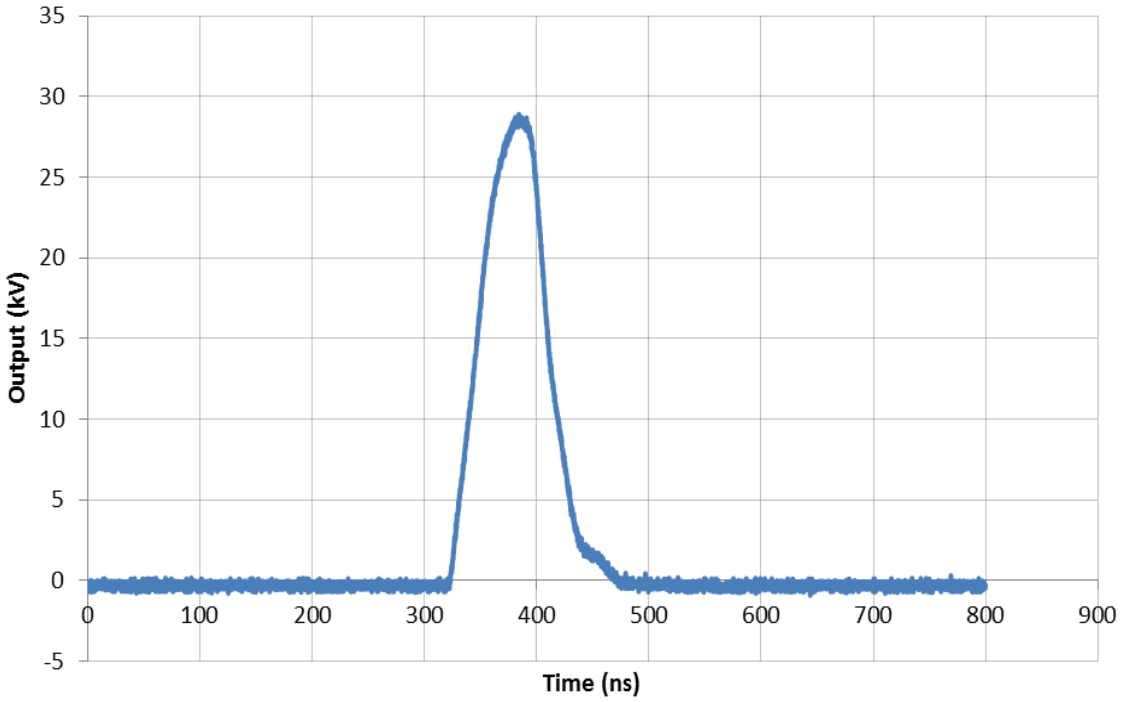

Fig. 3-5. LTD output when modules are switched in a same timing manner.

LTD output parameters: Output peak voltage ~ 29 [kV], Rise time 38 [ns], Fall time 37 [ns], FWHM 65 [ns], Pulse energy ~ 501 [mJ/pulse], Pulse No 1, Output power ~ 50 [W], Efficiency ~ 68%

3.1.2 30 Modules with Three Groups of Control Signals with Different Timing

In this experiment releasing of 3 groups of control signal with different timing and results is shown. Here control signals are released in 3 different timing groups and therefore LTD's output energy is divided in 3 parts. Each group of control signals is leading switching process of 10 LTD modules. Therefore LTD's output would be 3 pulses with energy of 10 modules (Fig. 3-6).

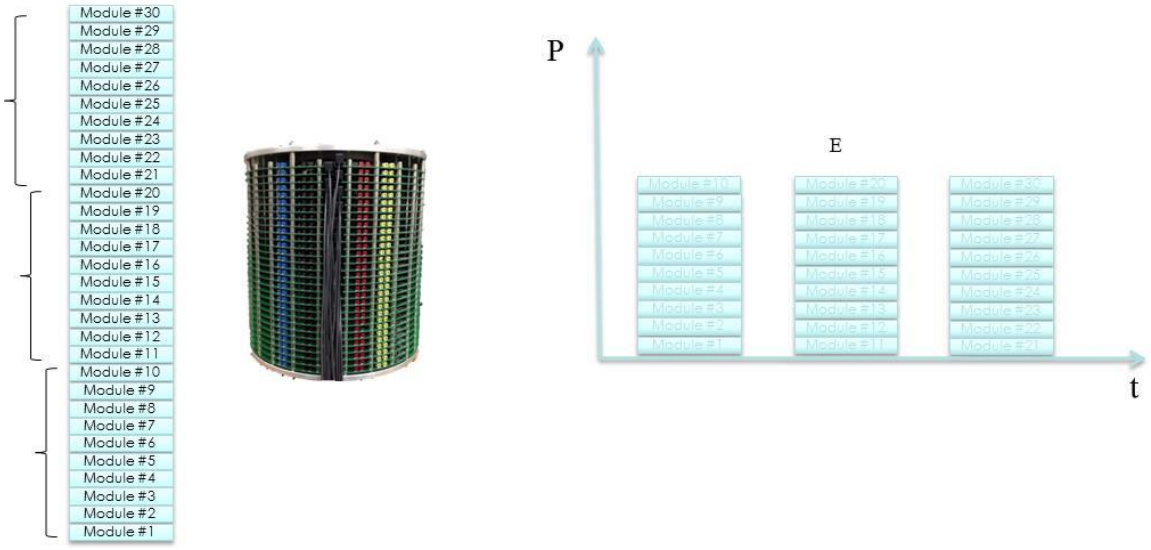

Fig. 3-6. LTD output energy illustration in a 3 different control signal timing.

In Fig. 3-7, LTD output in a system with 3 groups of control signal with different timing is shown.

LTD input parameters: Charging voltage 1 [kV], Input current 42 [mA], Frequency 100 [Hz], Pulse width 80 [ns], Resistance 117.5 [Ω], Input power 42 [W]

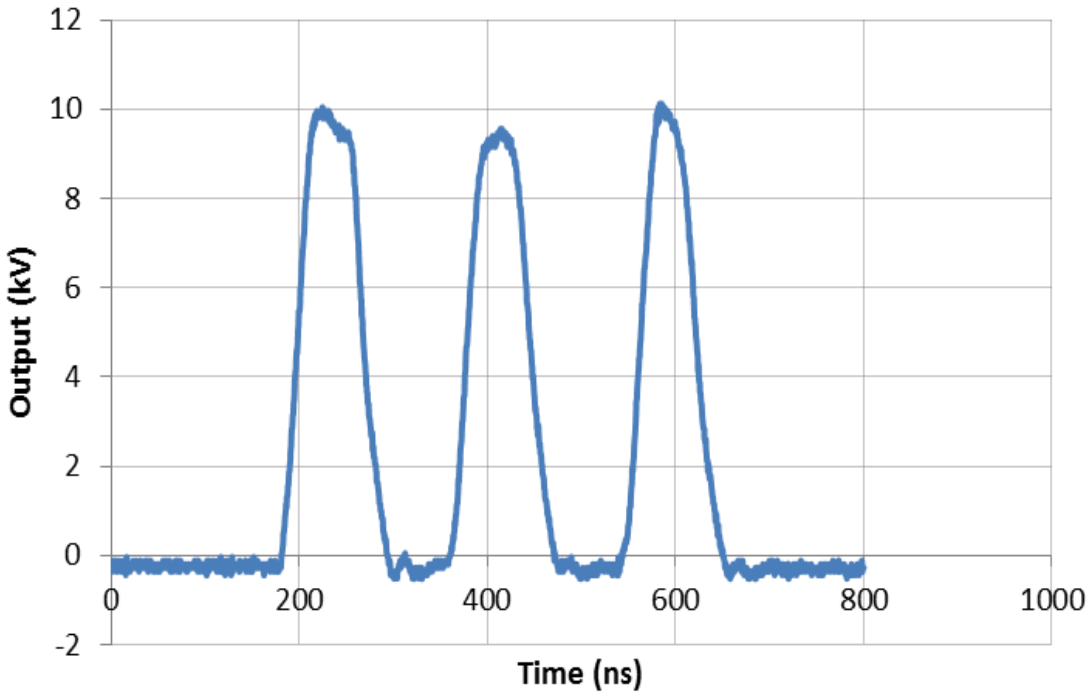

Fig. 3-7. LTD output with three group of control signal with different timing.

LTD output parameters: Output peak voltage ~10.12 [kV], Rise time 24 [ns], Fall time. 30 [ns], FWHM 72 [ns], Pulse energy 60[mJ/pulse], Pulse No 3, Output power 19 [W], Efficiency 45%

3.1.3 30 Modules with Arbitrary Control Signal Timing

This is an example of pulse shaping using FPGA-controlled LTD system. It shows that we can obtain an expected output voltage on the load by control of switching time of necessary number of modules. Here we have 3 different control signals group with different timing which control switching process of different modules. First group of control signals is leading 20 modules switching process; second and third group of control signals are leading switching process of 5 modules. We could obtain an output with 3 pulses with 20, 5 and 5 modules voltage amplitude. Arbitrary output would be obtaining by proper releasing of control signals for switching process (Fig. 3-8).

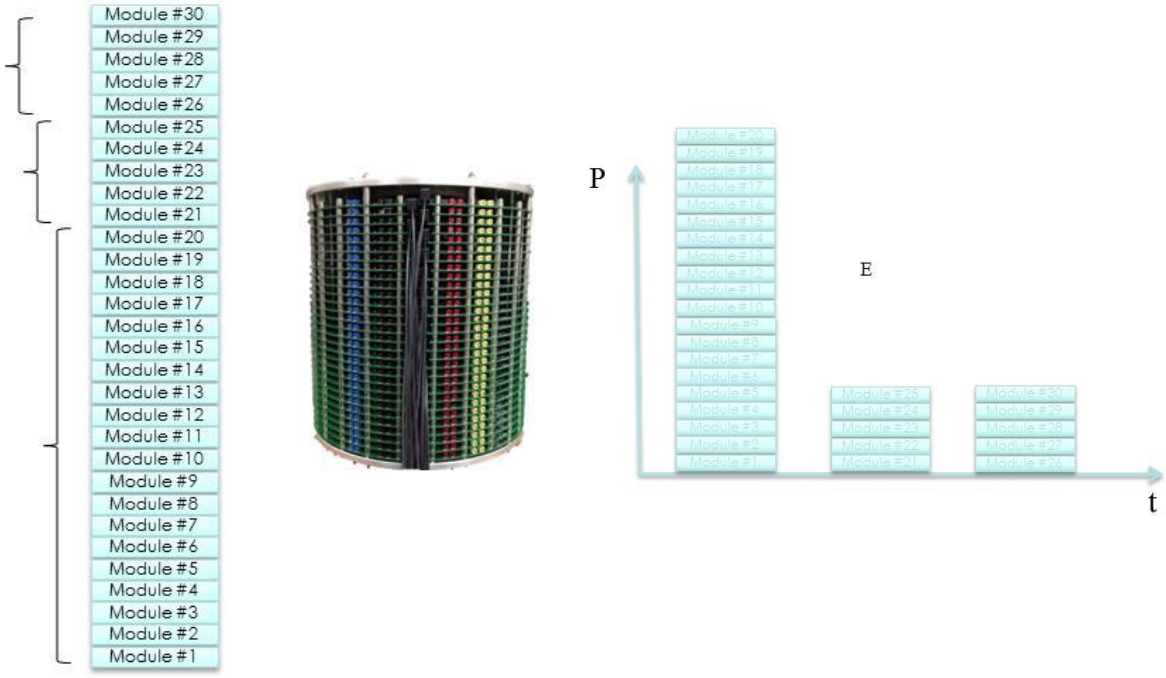

Fig. 3-8. LTD output energy illustration for desired pulses.

In Fig. 3-9, LTD output in a system with 3 groups of control signal for desired output pulses is shown.

LTD input parameters: Charging voltage 1 [kV], Input current 52 [mA], Frequency 100 [Hz], Pulse width 80 [ns], Resistance 117.5 [Ω], Input power. 52 [W]

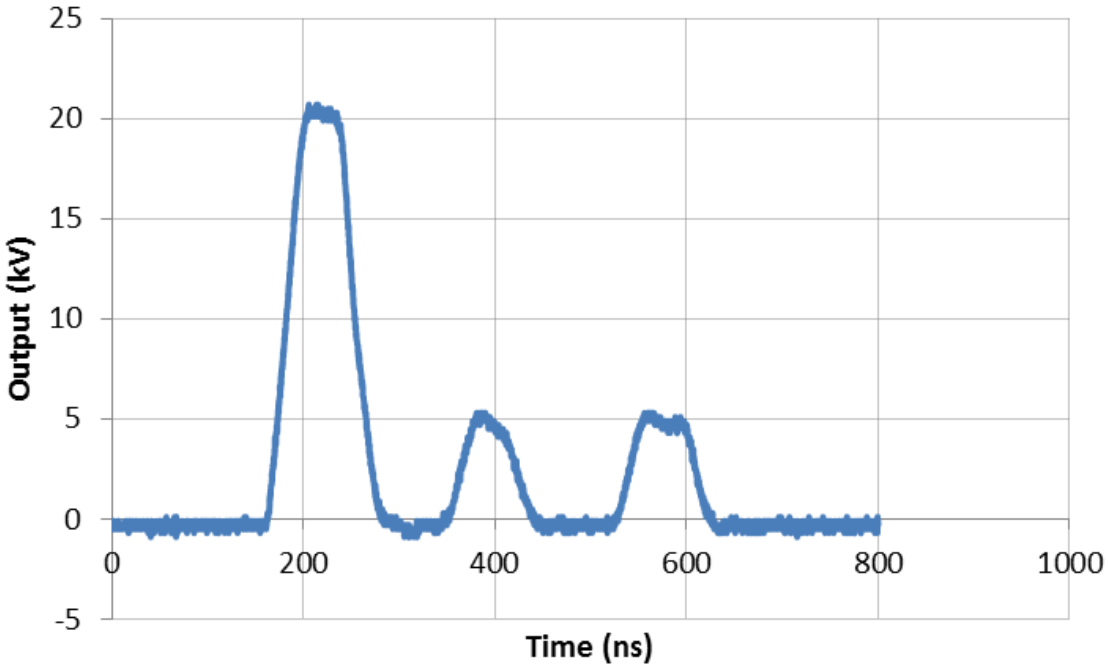

Fig. 3-9. LTD output for optional control signals timing.

LTD output parameters: Output peak voltage ~ 19.61 – 5.38 – 5.38 [kV], Rise time 29 – 21 – 21 [ns], Fall time. 32 – 24 – 24 [ns], FWHM. 71 - 74 - 74 [ns], Pulse energy. 232 – 17 – 17 [mJ/pulse], Pulse No. 3, Output power 23 – 2 - 2 [W], Efficiency 51%

3.1.4 LTD output for 10 Control of Control Signal with Different Timing

In the following experiments FPGA design is developed to produce 10 control signals groups for 30 modules of LTD. It means every 3 modules of LTD are controlled by one group of control signals with same timing. Therefore we could obtain an output with 10 pulses. Every pulse shows the output energy of 3 LTD modules. In Fig. 3-10, LTD output in a system with 10 groups of control signal with different timing is shown.

LTD input parameters: Charging voltage 1 [kV], Input current 32 [mA], Frequency 100 [Hz], Pulse width 80 [ns], Resistance 117.5 [Ω], Input power 32 [W]

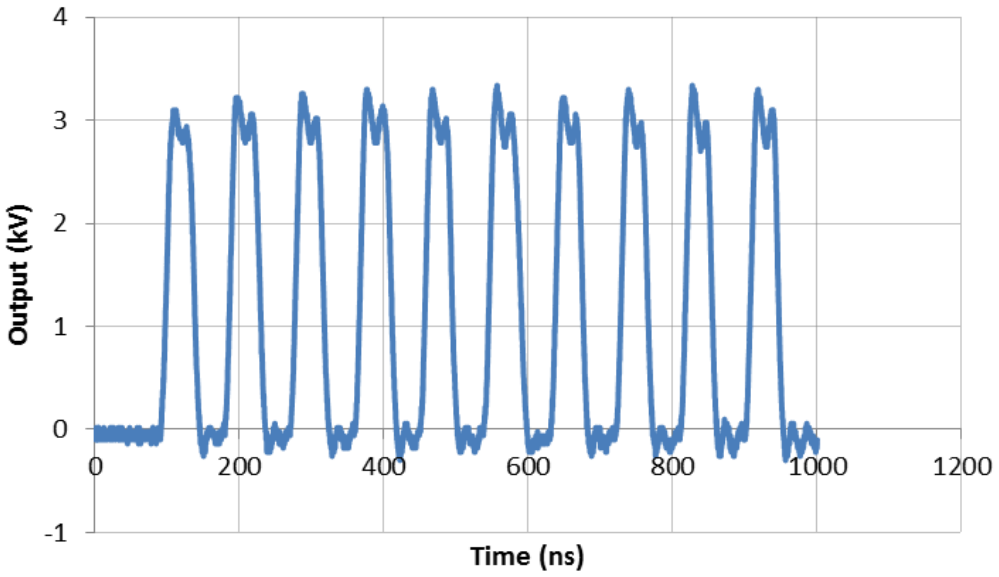

Fig. 3-10. LTD output for 10 groups of control signals with different timing.

LTD output parameters: Output peak voltage ~ 3.26 [kV], Rise time 21 [ns], Fall time. 21 [ns], FWHM 71 [ns], Pulse energy 6 [mJ/pulse], Pulse No 10, Output power 6.5 [W], Efficiency 20%

3.1.5 LTD Output for 15 Groups of Control Signal with Different Timing

In the following experiments FPGA design is developed to produce 15 control signals group for 30 modules of LTD. It means every 2 modules of LTD are controlled by one group of control signals with same timing. Therefore we could obtain an output with 10 pulses. Every pulse shows the output energy of 2 LTD modules. In Fig. 3-11, LTD output in a system with 15 groups of control signal with different timing is shown.

LTD input parameters: Charging voltage 1 [kV], Input current 32 [mA], Frequency. 100 [Hz], Pulse width 80 [ns], Resistance 117.5 [Ω], Input power 32 [W]

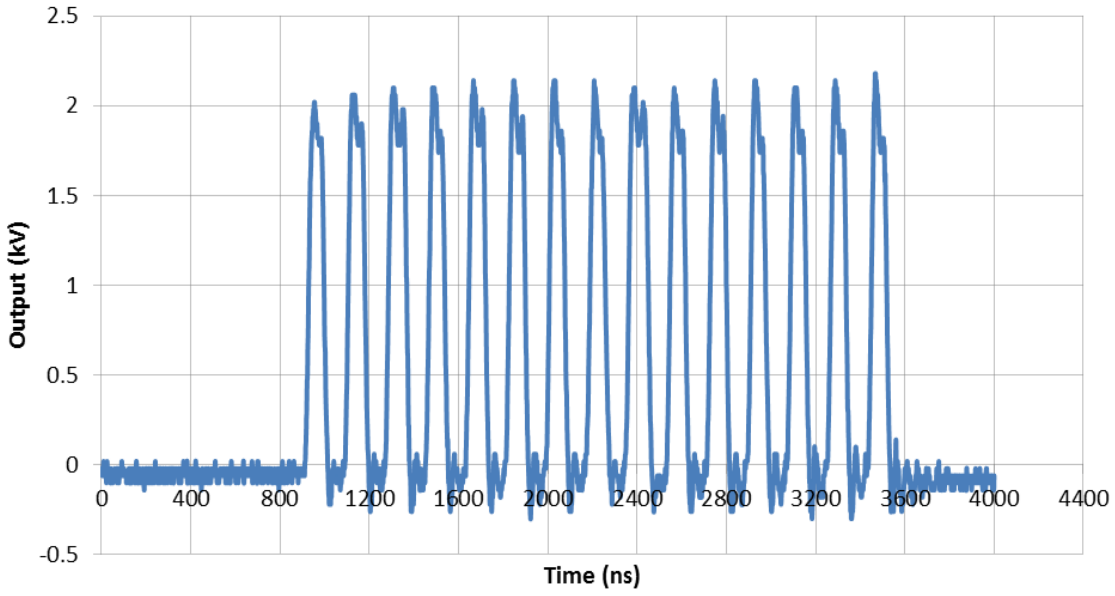

Fig. 3-11. LTD output for 15 groups of control signals with different timing.

LTD output parameters: Output peak voltage ~ 2.18 [kV], Rise time 21 [ns], Fall time. 21 [ns], FWHM 71 [ns], Pulse energy 3 [mJ/pulse], Pulse No 15, Output power 4.31 [W], Efficiency. 13%

3.1.6 LTD Output for Control Signal with Different timing for 30 Modules

In this experiment modules are switched at different timings, their output voltages are still added up on the axis of time. This is proved by switching all 30 modules at different times from one another, generating a burst of 1-kV output pulses, one by each module, as shown in Fig. 3-12.

LTD input parameters: Charging voltage 1 [kV], Input current 29 [mA] Frequency. 100 [Hz], Pulse width 80 [ns], Resistance 117.5 [Ω], Input power 29 [W]

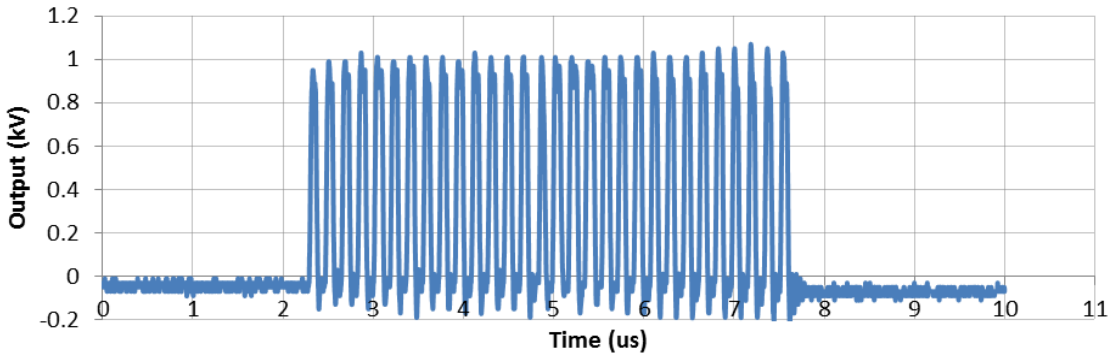

Fig. 3-12. LTD output for 30 control signals with different timing.

LTD output parameters: Output peak voltage ~ 1 [kV], Rise time 24 [ns], Fall time. 23 [ns], FWHM 70 [ns], Pulse energy 1 [mJ/pulse], Pulse No. 30, Output power 2 [W], Efficiency 7%.

3.1.7 Efficiency Analysis

The total switching current is higher than the load current due to eddy current loss of the magnetic core. In this part switching current in different situation (timing group of control signals) has been measured and compared with load current. The difference between switching current and load current considered to be the eddy current loss of the core which flowed through the cavity case and shown as Rc. It is appeared in parallel to a load resistor during discharge as it is shown in Fig. 3-13.

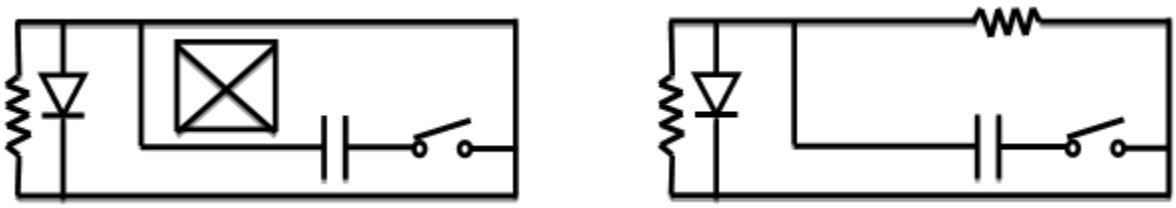

(a) (b)

Fig. 3-13. (a) Equivalent circuit of a module, (b) Same circuit which is showing the equivalent total core resistance Rc as parallel to Rload.

$$R_C = k\frac{\rho S}{\delta^2 \ell}$$

ρ: resistivity of the core
S: total cross-sectional area of the core
k: dimensionless coefficient
d: thickness of iron tape
ℓ: the circumference of the core

For example when there is only one group of modules and all of modules are being switched ON and OFF at the same time, In repetitive operation of 100 Hz with charging voltage of 1 kV, the average Input current is measured to be ~ 74 mA, with which we find the discharge coulomb of 74 μC/pulse. Then, with the pulse width of 70 ns, the average

discharge current during each pulse is estimated to be ~352 A. The difference between this value and the load current of ~ 247 A is considered to be the eddy current loss of the core, which flowed through the cavity case. It is assumed that the eddy current loss of the magnetic core can be represented by an equivalent resistor of Rc. In this case, our experimental results have indicated a value of Rc ~257-Ω for the core we have used, which is in parallel with our load resistor of 117.5 Ω. Consequently, the total discharge current is calculated to be ~365 A for output voltage of ~29 kV.

The peak Output power to the 117.5-Ω load reaches ~7.15 MW with output energy of ~ 0.49 J/pulse. At a pulse repetition rate of 100 Hz, the charging current of the primary power supply reached~74 mA, giving an input power ~ 74 W. A system efficiency is therefore obtained to be ~68% by dividing the average Output power by the input power. But in case of multiple output pulses which cause lower output voltage, efficiency will decrease.

But when all modules are being switched in different timing, for the same charging voltage of 1 kV and Input current of 29 mA, input power is ~ 29 W. With 1 kV output voltage the Output power reaches to ~ 8.5 KW with output energy of 0.58 mJ/pulse and at the repetition rate of 100 Hz in presence of 30 pulses output energy will be ~2 J. This gives a system efficiency of ~ 7%. Therefore we can say that when the load impedance is constant, the system efficiency decreases for lower output voltage. The reason is that, for lower output voltage, the output current decreases, while the magnetizing loss on the core is nearly proportional to the operation voltage of each module.

In Fig. 3-14, output Pulse energy and its relation to efficiency are shown. As it is shown when output voltage decrease the system efficiency also decrease.

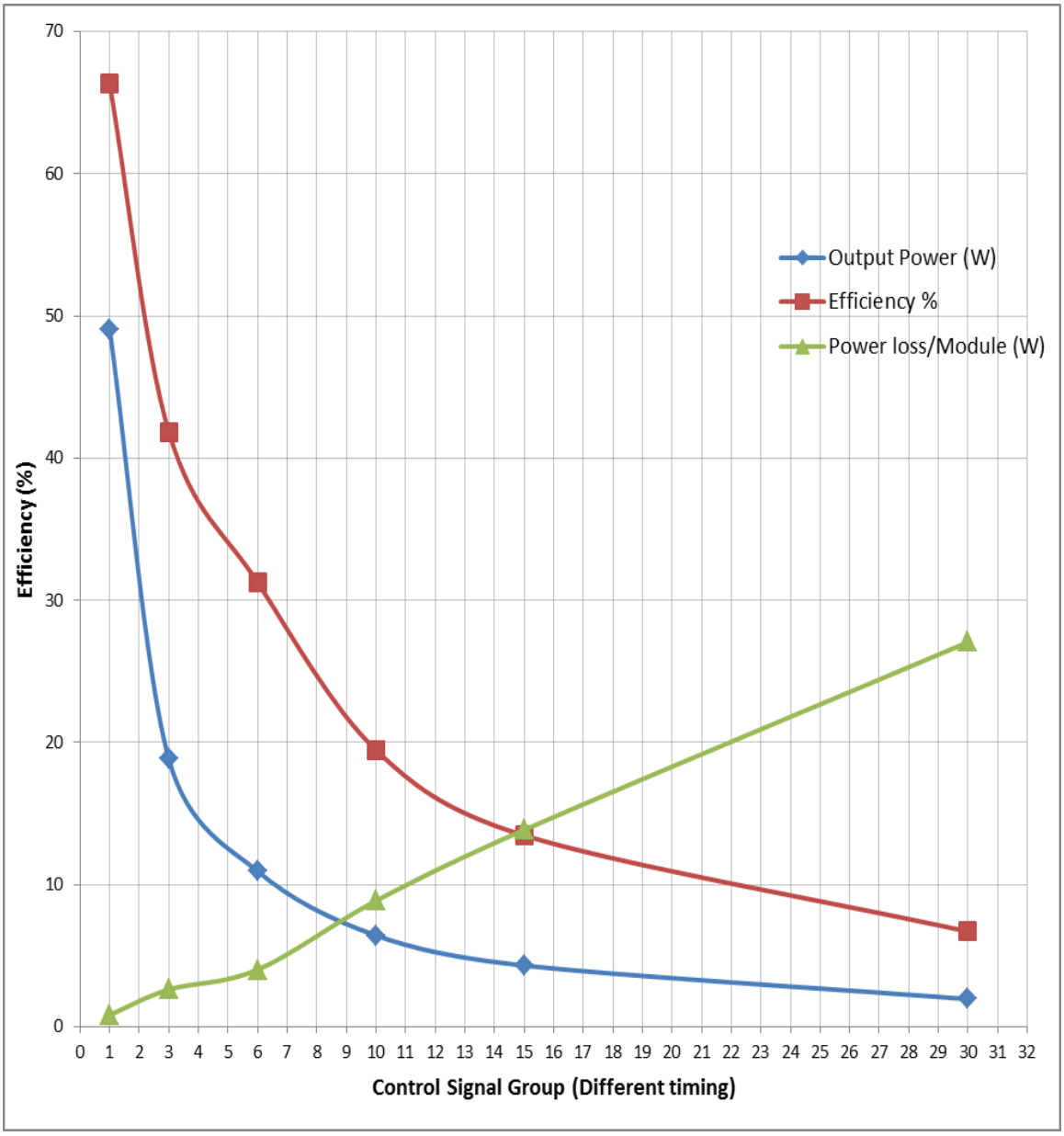

Fig. 3-14. Efficiency and control signal group relation.

4 CHAPTER IV: WAVEFORM CONTROL OF ATMOSPHERIC PREASSURE DISCHARGE USING LTD

4.1 Overview

Pulsed atmospheric discharge has potential applications to plasma generation for many kinds of industrial processes. It is considered to be more flexible and more efficient compared with conventional RF or microwave discharge. It can omit dielectric barrier, which is essential for continuous high frequency discharge to prevent arc transition, by using very short pulse that does not give the arc enough time to develop. Pulsed atmospheric discharge is characterized by its time-varying impedance, which is a result of rapid plasma development between the electrodes. This study is going to explain a new method which allows us to adjust the applied voltage properly and control the discharge current behavior and keep it in a certain extent.

4.2 Waveform Control of Atmospheric Discharge

Discharge process begins with creating high electric field near to the main electrode. At the beginning, a very high voltage is required to cause a breakdown in the cold gas and to initiate a discharge current. However, if this voltage amplitude is sustained, it will expand the discharge plasma and quickly form a low impedance channel between the electrodes. So far, the most typical way of avoiding this impedance collapse is to terminate the applied voltage and finish the pulse before the current gets out of control. It

is clear that properties of the discharge plasma highly depend on the characteristics of the input voltage pulses, i.e., voltage amplitude, pulse width and rise time. By using the solid-state LTD pulse shaping advantage (Fig. 4-1), we can expect a certain level of current control by adjusting the applied voltage amplitude without terminating it. The basic consideration is that an increase in voltage tends to increase the discharge current, while a decrease in voltage tends to decrease the current. Therefore, in principle, we can adjust the discharge current by varying the applied voltage. In other words, by synthesizing a proper voltage waveform, we can create an arbitrary current waveform for a given discharge load.

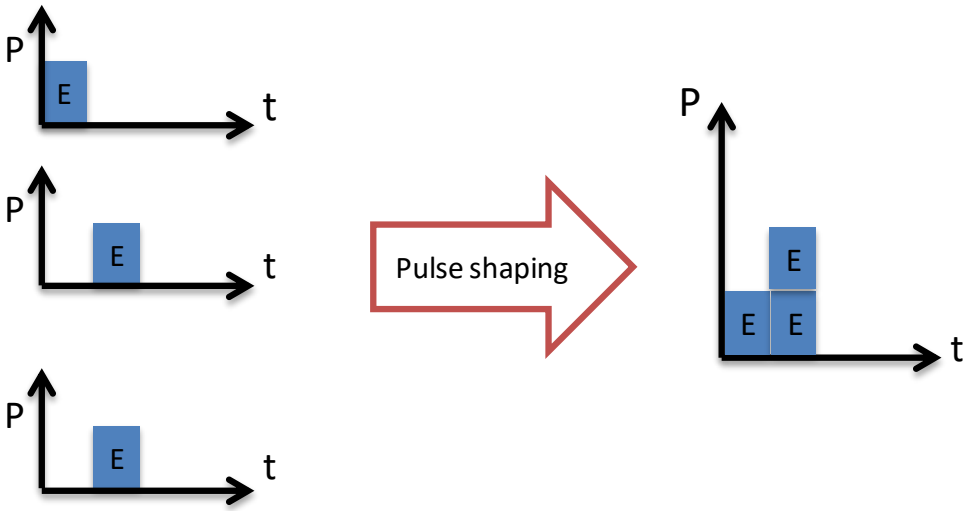

Fig. 4-1. Pulse shaping for arbitrary control.

4.2.1 Experimental Setup

As an example to demonstrate the pulse shaping using LTD, we have used our LTD stack to drive the atmospheric discharge between a wire and a coaxial cylinder. The copper wire has a diameter of 1 mm, and it is 10 mm away from the stainless steel outer conductor. Load picture and its schematic are shown in Fig. 4-2. Experimental picture is shown in Fig. 4-3.

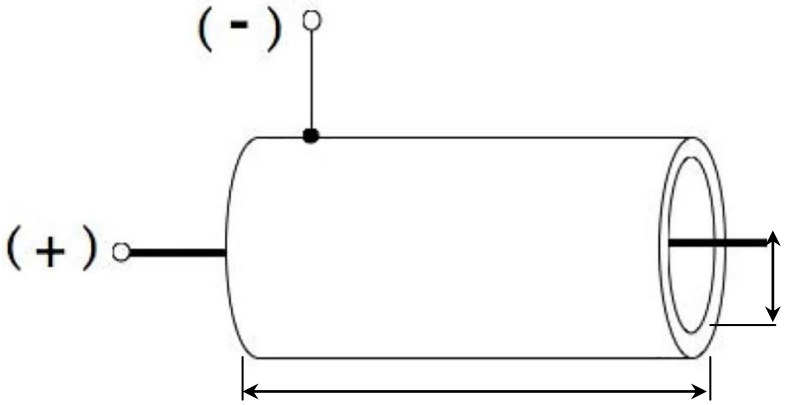

(a)

(b)

Fig. 4-2. (a) Atmospheric discharge load configuration. (b) Load picture.

Fig. 4-3. Experimental setup.

4.2.2 Phenomena Observation

As the first experiment a voltage pulse of 15 kV, 40 ns applied to the load. Output voltage is shown in Fig. 4-4. As it is observable, when the applied voltage pulse is short, the discharge current is relatively low and stays in a certain level.

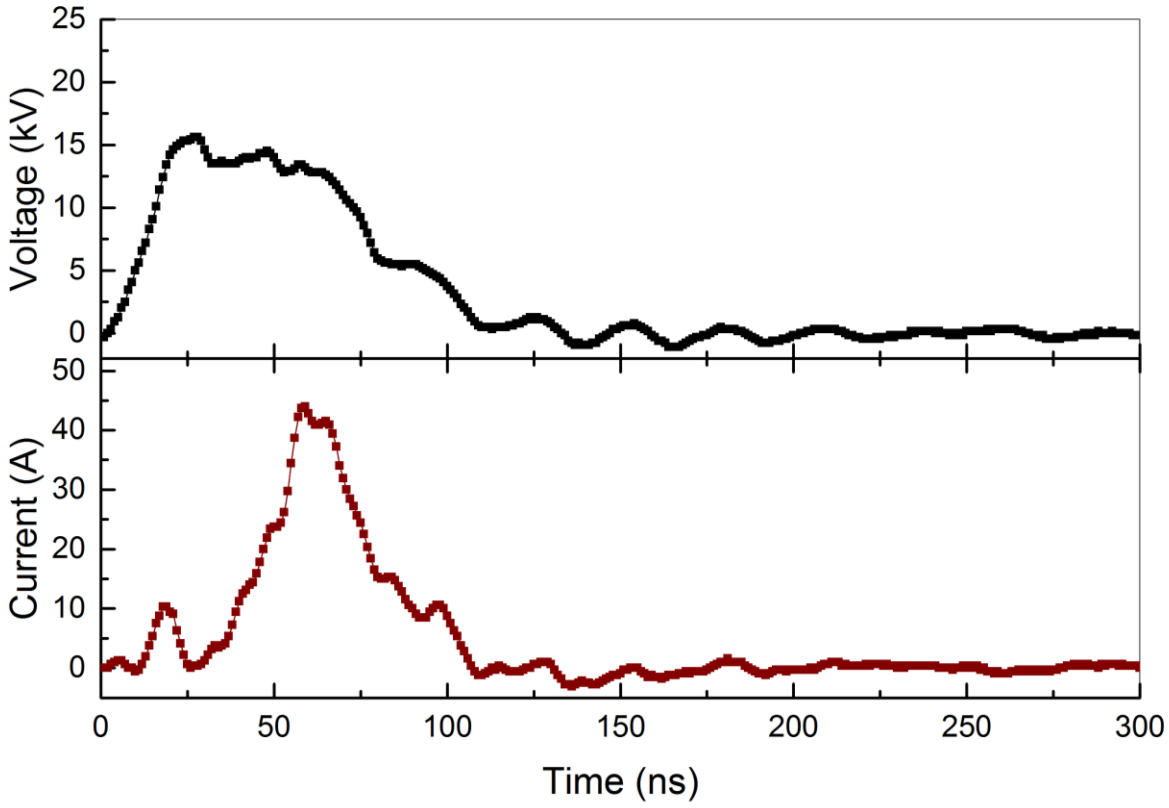

Fig. 4-4. Load voltage and current waveform when applied voltage is 15 kV, 40 ns.

When same voltage arrangement is applied in a longer period of time, 15 kV, 100 ns, the discharge current increases significantly due to plasma development near the center electrode (Fig. 4-5).

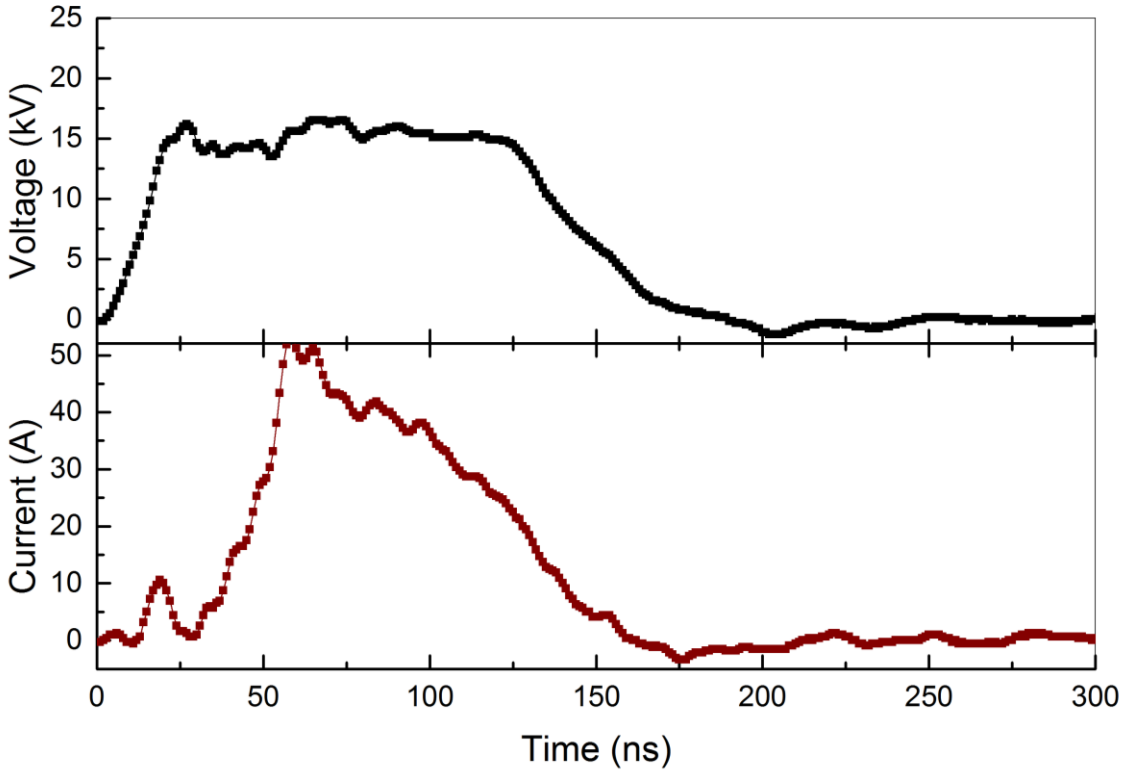

Fig. 4-5. Load voltage and current waveform when applied voltage is 15 kV, 100 ns.

Therefore, to suppress the peak load current, we can decrease the load voltage for the later part of the pulse. It is obvious that the high-voltage spike at the beginning is necessary to initiate the breakdown. However, sustaining the discharge usually requires a lower voltage, and our LTD stack is a perfect generator to shape the voltage pulse. The following experiments are good example of this kind of adjustment method.

4.2.3 Current Waveform by Voltage Adjustment, 40 A, 100 ns

Fig. 4-6, shows a typical result obtained when the discharge current was aimed at constant value of 40 A. It was obtained by manually adjusting the LTD control signals, through FPGA, without changing LTD charging voltage. This result gives a relatively constant discharge current near 40 A which lasted for more than 100 ns.

From Fig. 4-6, we see that 18 modules were turned ON at the beginning, which is required to initiate the gas breakdown and to bring the discharge current to ~ 40 A. After 40 ns, three modules were turned OFF in order to avoid current overshooting. However, since the remaining output voltage is apparently not enough to sustain a constant current, appropriate numbers of LTD modules were switched ON at appropriate times, resulting in nearly constant discharge current.

It should be noted that in this kind of control method, there is no need for any change in hardware of system. As it was showed, all the voltage adjustment is being done with FPGA and its control signals.

Similar experiments have been carried out for targeting current at 30, 20, and 10 A, and the results are shown in the Figures 4-7, 4-8 and 4-9 respectively.

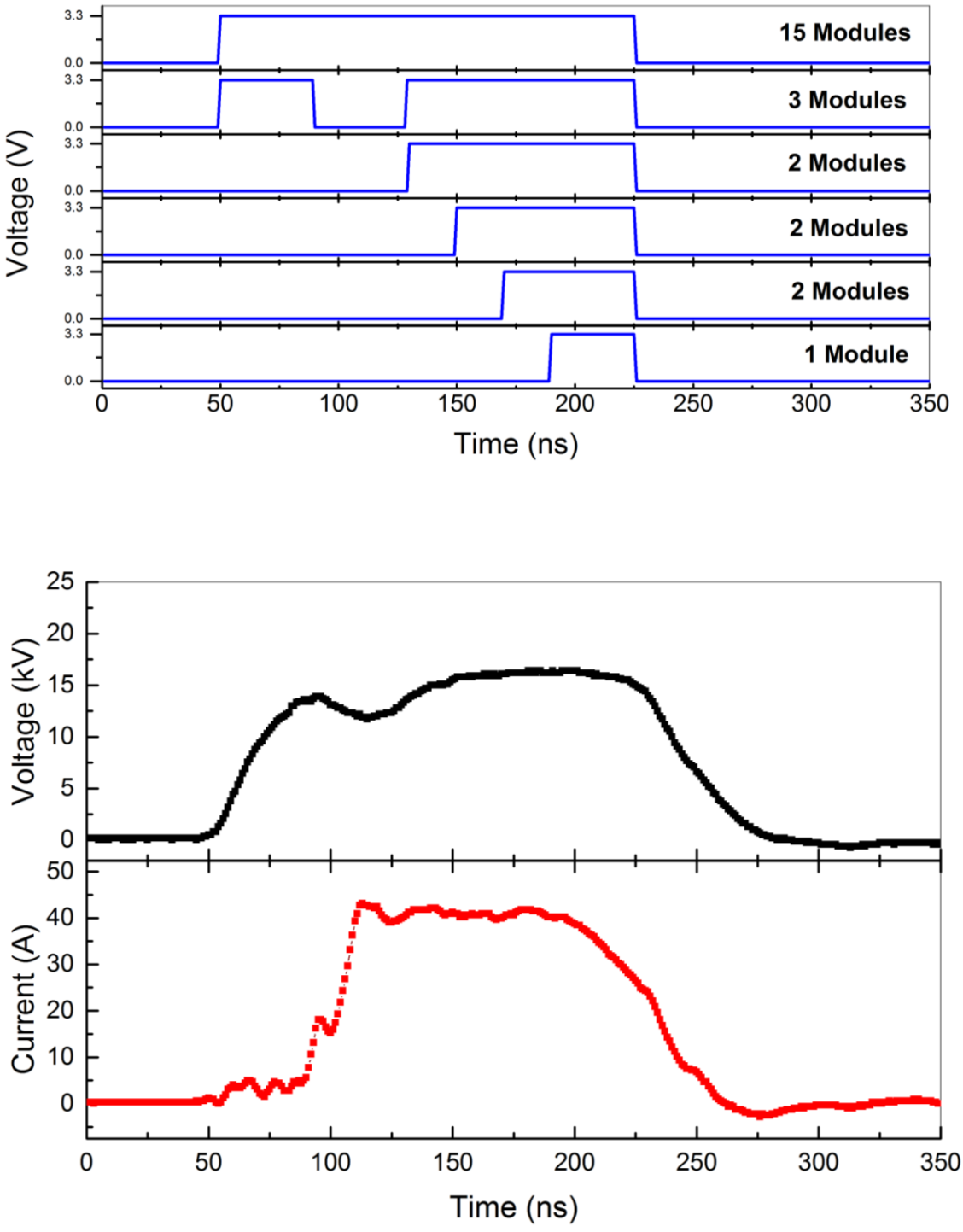

Fig. 4-6. (a) Time variation of LTD control signals. (b) Waveforms of load voltage and current, obtained with LTD charging voltage of 734 V.

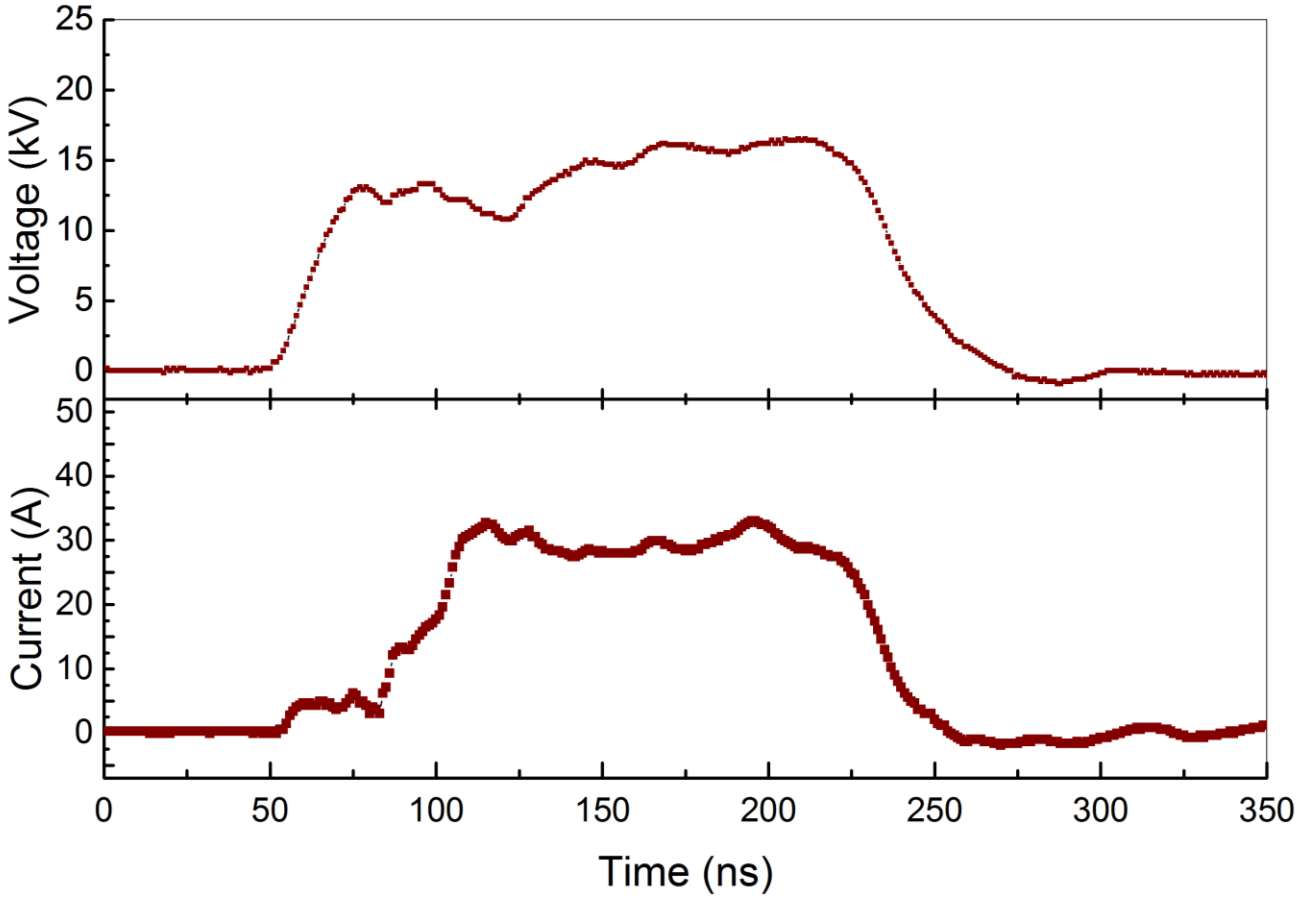

Fig. 4-7. Waveforms of load voltage and current, obtained with LTD for 30 A targeted current.

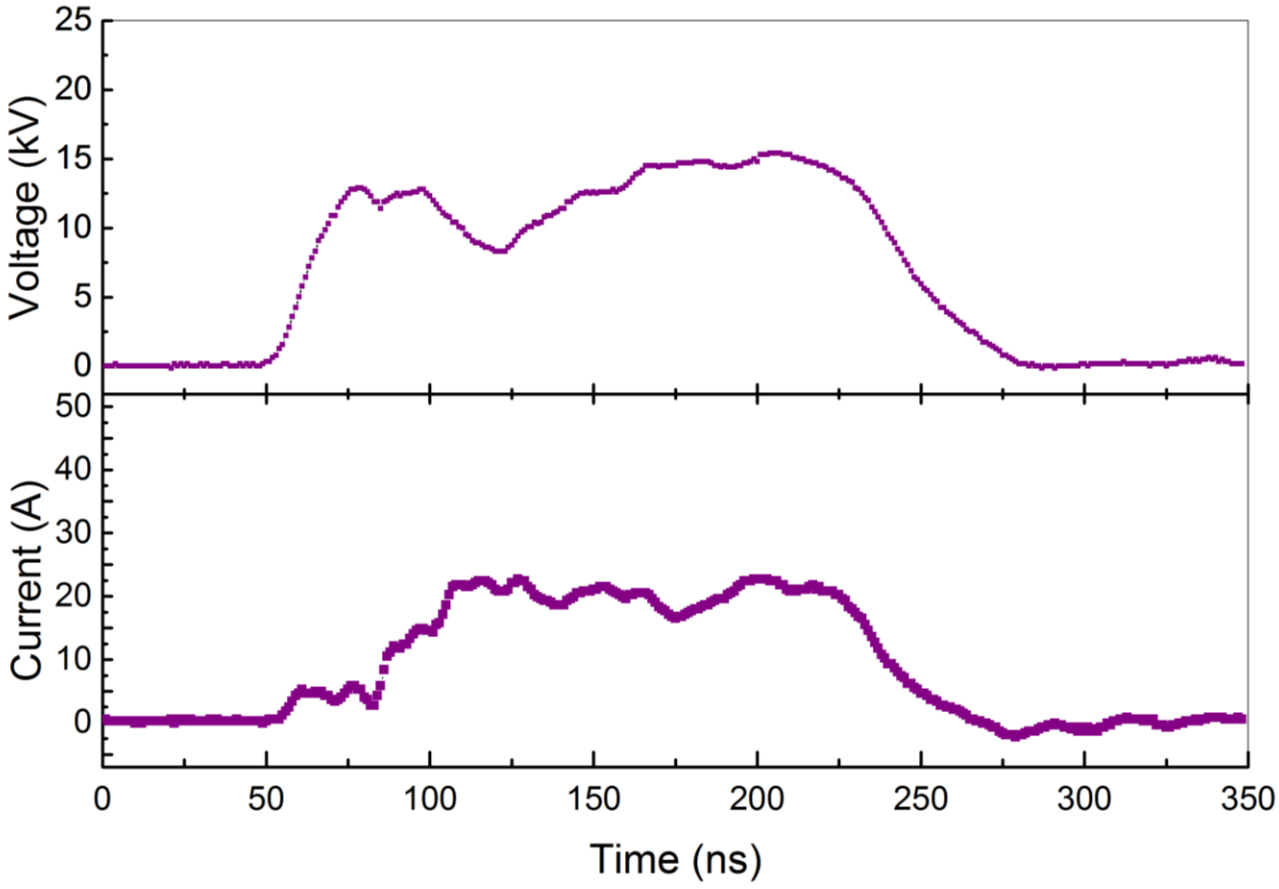

Fig. 4-8. Waveforms of load voltage and current, obtained with LTD for 20 A targeted current.

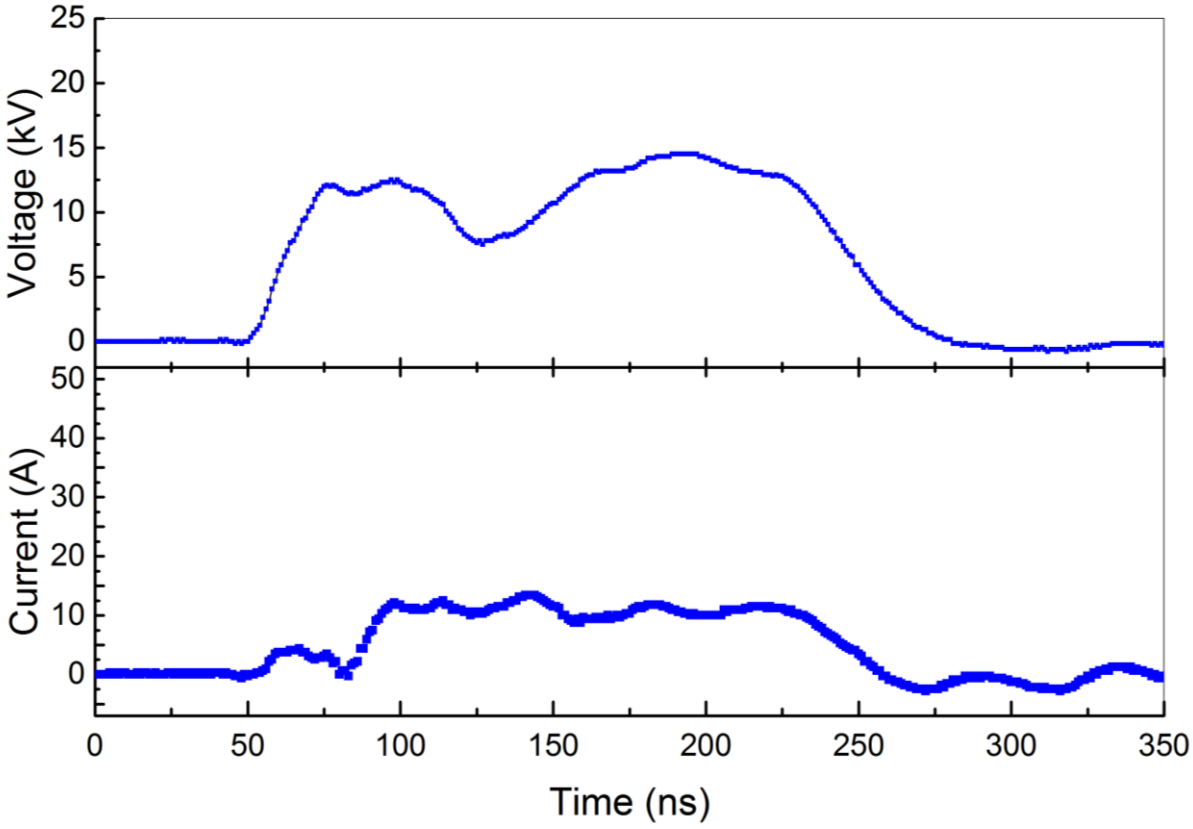

Fig. 4-9. Waveforms of load voltage and current, obtained with LTD for 10 A targeted current.

4.2.4 Atmospheric Discharge Load Impedance Analysis

Gas discharge under atmospheric pressure is characterized by its dynamic impedance variation. In the other word, time-varying impedance behavior is one of their specifications. So far we have shown that with a well-controlled time history of the applied voltage we can control the discharge current of the load. In Fig. 4-10, load impedance waveform, dividing the voltage with the current is shown for each targeted current. It can be seen the load impedance is controlled in a certain level.

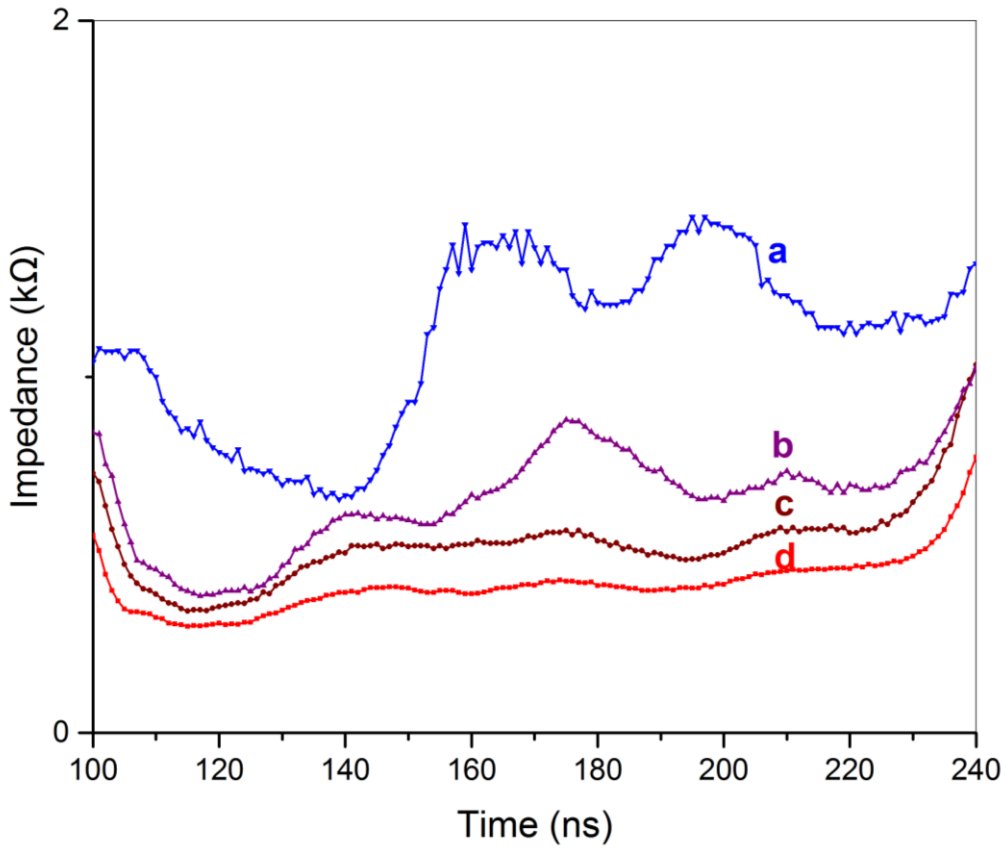

Fig. 4-10. Corresponding load impedance seen from LTD, obtained while aiming the current at (a) 10A, (b) 20A, (c) 30A, and (d) 40A, respectively.

4.2.5 Flexible Current Control, Step up

In this experiment using the by carrying out delicate voltage waveform adjustment, we tried to “draw” the current curve in a way that we wish. We have released the control signals of FPGA to have a step-up current from ~10 A to ~30 A.

Result is shown in Fig 4-11. As control signals show, at the ending part of the pulse where we need a higher discharge current most of module are ON.

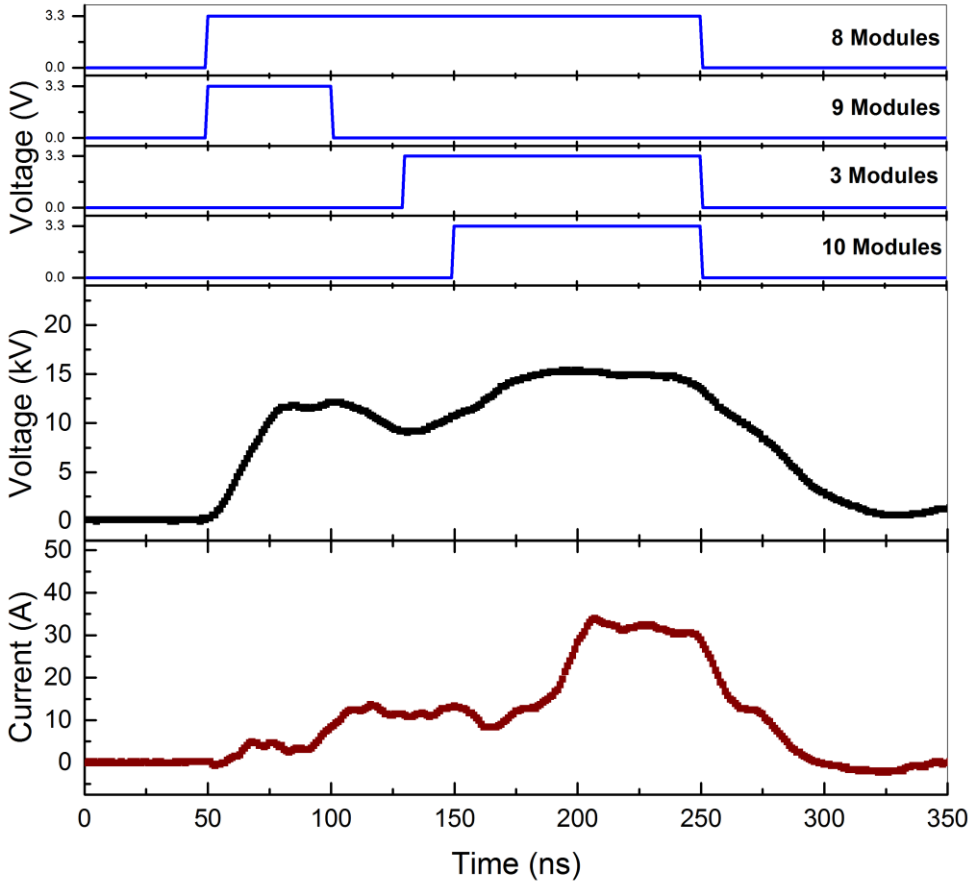

Fig. 4-11. Control signals of FPGA and Voltage and Current waveform of load in ~10 A to ~30 A step-up current control.

4.2.6 Flexible Current Control, Step down

In Fig. 4-12 LTD modules are switched ON and OFF for a step-down current drawing. As it can be seen, current will decrease form ~30 A step to ~ 10 A step.

This current drawing is being done only by FPGA control signal adjustment. It could be count as a creditable advantage because there is not any need for hardware change for desired output.

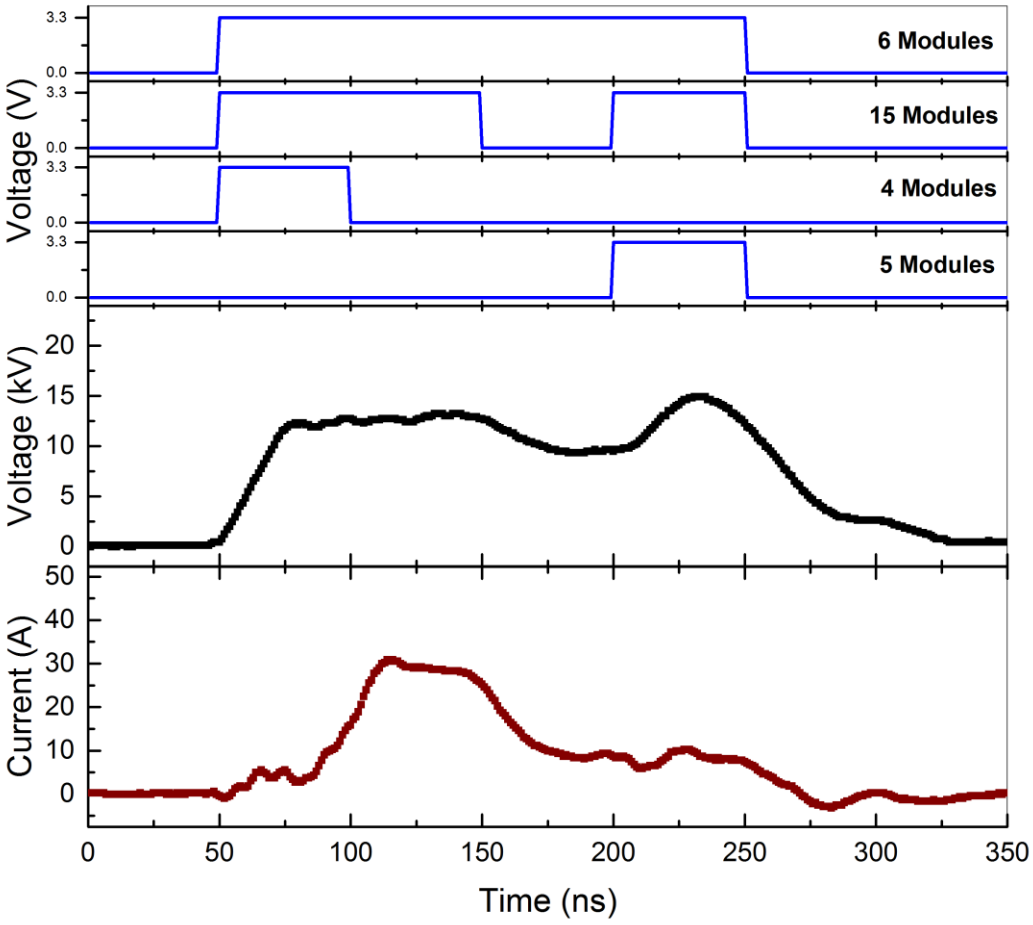

Fig. 4-12. Control signals of FPGA and Voltage and Current waveform of load in ~30 A to ~10 A step-down current control.

5 CHAPTER V: STUDY OF ATMOSPHERIC DISCHARGE BY USING LTD

5.1 Overview

Pulsed Atmospheric discharge is known for its activity in generating large amount of radicals that are being used in environmental, medical, and biological applications. Compared with other gas discharge processes, such as radio-frequency or microwave discharge, pulsed atmospheric discharge is characterized by its flexibility and controllability. In addition, it can omit the dielectric barrier which is sometimes considered as a very essential component for gas discharge apparatus.

Pulsed atmospheric discharge usually starts from spatially partial breakdown initiated by electric field concentration due to the electrode geometry. The discharge sends streamers to a much wider area between the electrodes resulting in volumes of active species. The number and the behavior of the streamers depend very much on the amplitude and the rise-time of the electric field. In addition, depending on the external circuit, the development of the streamers may affect the temporal variation of the amplitude of the applied voltage.

When using pulsed atmospheric discharge for plasma radical production, as it has been expected by many industrial applications, it is important to maintain a certain level of the electric-field intensity in order to achieve effective acceleration of the electrons. On the other hand, gas discharge under relatively high pressure tends to migrate toward plasma

channel formation which significantly increases the conductivity of the medium and lowers the gap voltage due to circuit effect. This problem is usually dealt with by keeping the voltage pulse short enough so that the discharge is terminated before the load impedance collapses. Therefore, the performance and efficiency of pulsed atmospheric discharge depend on the output characteristics of pulsed voltage generator.

We have developed a relatively new type of pulsed voltage generator by using a circuit scheme called linear transformer driver (LTD). It has been proved to be unique in output flexibility especially on waveform control. We have tested the LTD-type pulsed voltage generator with a pair of coaxially configured electrodes and demonstrated load impedance control by carrying out voltage waveform control.

In this chapter, we have used our LTD-type pulsed voltage generator to study the influence of a pulsed atmospheric discharge on the behavior of the following pulse for consecutive operation. Since applications of pulsed atmospheric discharge require repetitive operation, it is always important to know and to understand the effect a pulsed discharge can create in the gas that may result in different behavior of the next pulse following it.

5.2 Experimental Phenomena

The discharge load is the same as that we have used in the previous experiments. As shown in Fig. 5-1 (a), it consists of a pair of coaxially configured electrodes, a wire of 1 mm in diameter and a pipe of 20 mm in inner diameter. Both are made of stainless steel with length of 320 mm. The pulsed power source applies positive voltage on the wire so that discharge occurs in the region near the wire, as seen in Fig. 5-1 (b).

The pulsed high voltage is generated by using an LTD-type generator. It consists of many modules and it generates pulsed high voltage by adding the output voltage of all modules through pulse transformers. Each module is formed by many unit circuits connected in parallel, each of which consists of a capacitor and a switch. The basic concept of LTD is that it generates pulsed power by synchronizing many small pulses and by adding them together both voltage-wise and current-wise. This scheme is significantly different from traditional approach where short pulse of relatively high power is generated by compressing a long pulse of relatively low power.

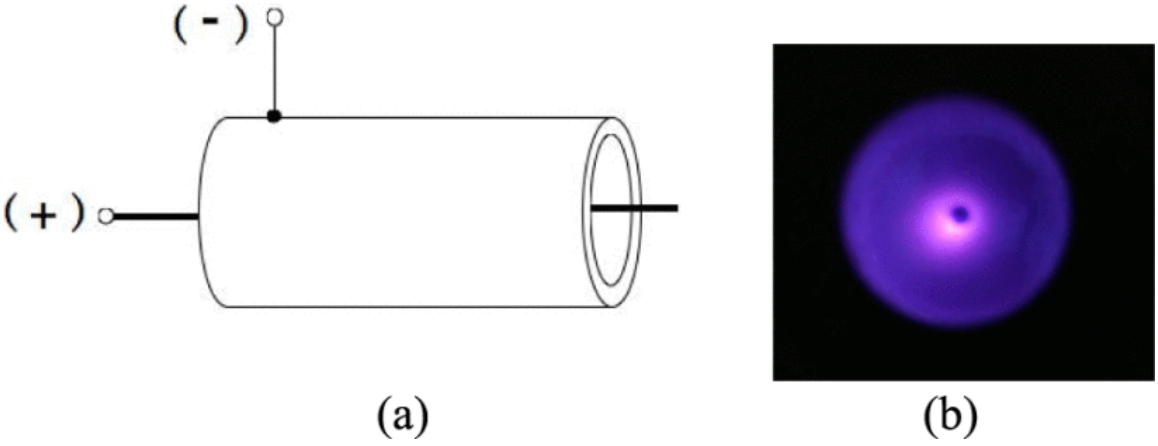

Fig. 5-1. (a) Electrode's configuration. (b) Time integrated end-view photograph.

Experimental setup is shown in Fig. 5-2. The LTD system used in this experiment has been reported in previous chapters. It has 30 modules and each module has 24 unit circuits that use MOSFETs as switches. It is capable of generating pulsed voltage up to 30 kV with maximum current of 300 A, and pulse length variable in the range of 60~200 ns. By properly switching different modules, we can easily change the output voltage and the interval between consecutive pulses, as we need to do for the following experiments.

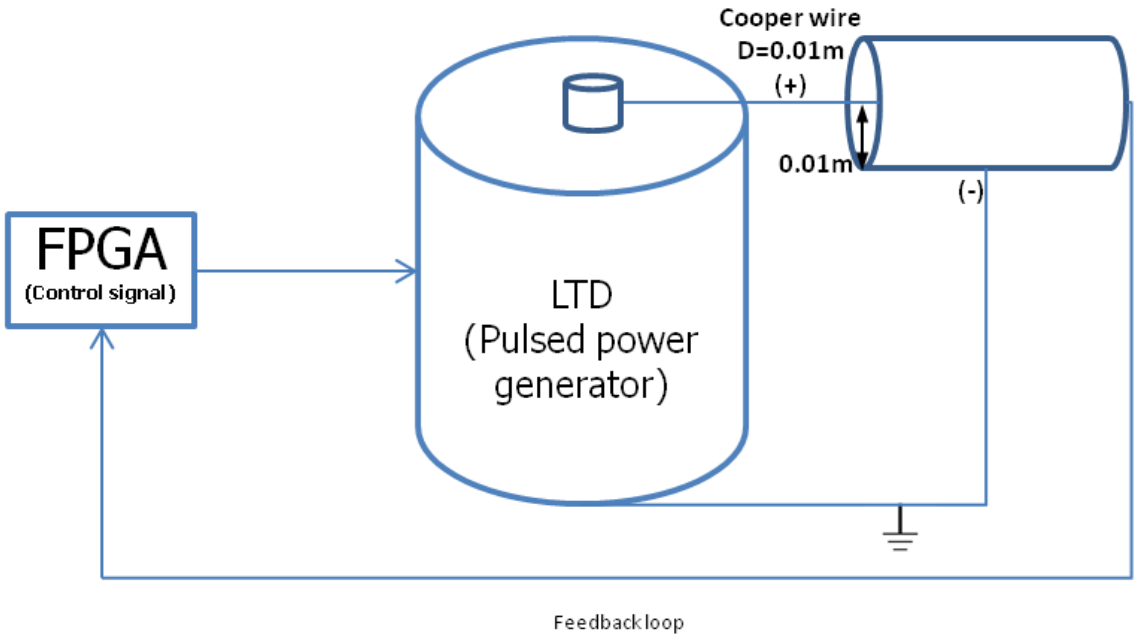

Fig. 5-2. Experimental setup for study on consecutive operation of Atmospheric Discharge.

5.2.1 Two Consecutive 15 kV, 50 ns Pulse with Time Interval of 150 ns

We applied the output voltage of the LTD to the discharge load. When the voltage amplitude is above a certain value, a discharge current can be observed. Fig. 5-3 shows the waveforms of voltage and current, when two almost identical voltage pulses were applied with a time interval of 150 ns. However, a difference in the discharge current is clearly identified. From Fig. 5-3, we can see that the peak current of the second pulse is evidently lower than that of the first pulse.

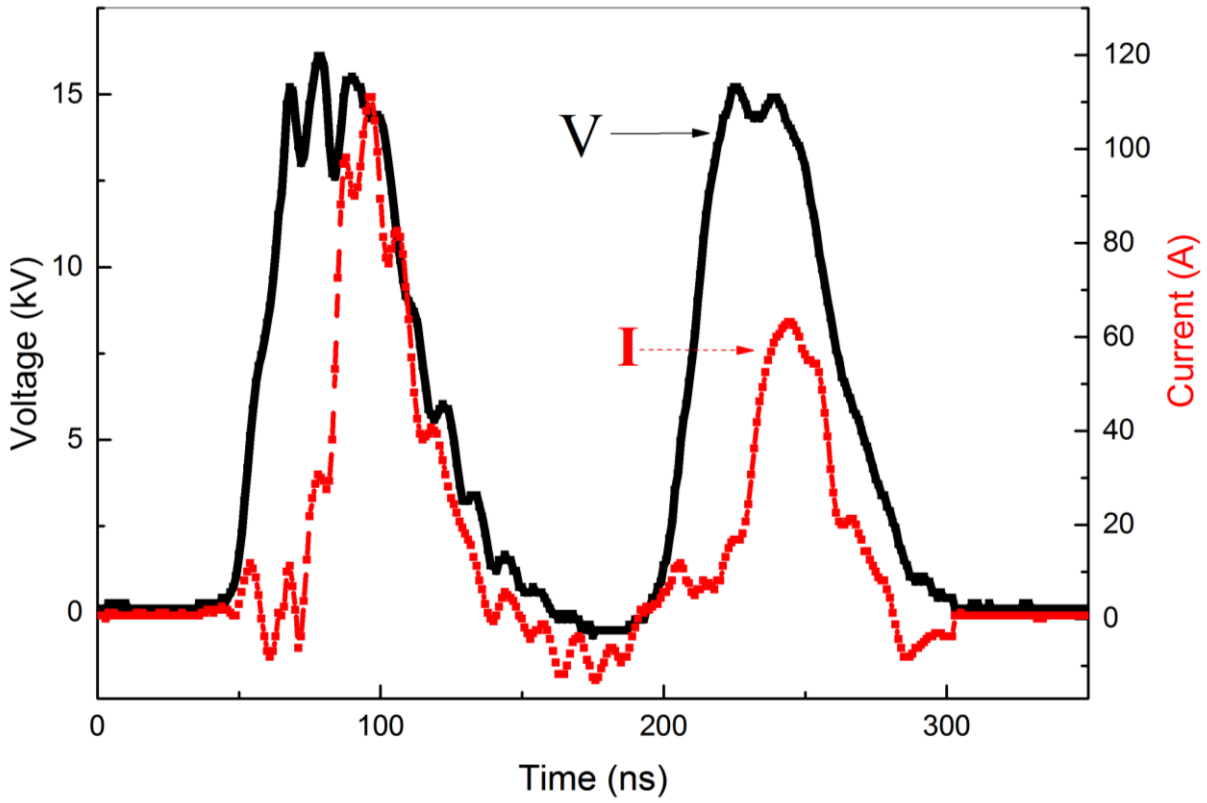

Fig. 5-3. Voltage and current waveforms for double pulse discharge with interval of 150 ns, for about same voltage amplitude.

5.2.2 Voltage Adjustment for Same Current Peak

Considering the current leakage in the second pulse in pervious experiment, to identify the phenomena we have increased the amplitude of the second pulse until its peak current reaches that of the first pulse, and the result is shown in Fig. 5-4. These results show that there is a difference in the initial state, between two pulses, when the voltage is applied. In other words, the first pulse has caused a change in the gas state so that the second discharge behaved differently from the first one.

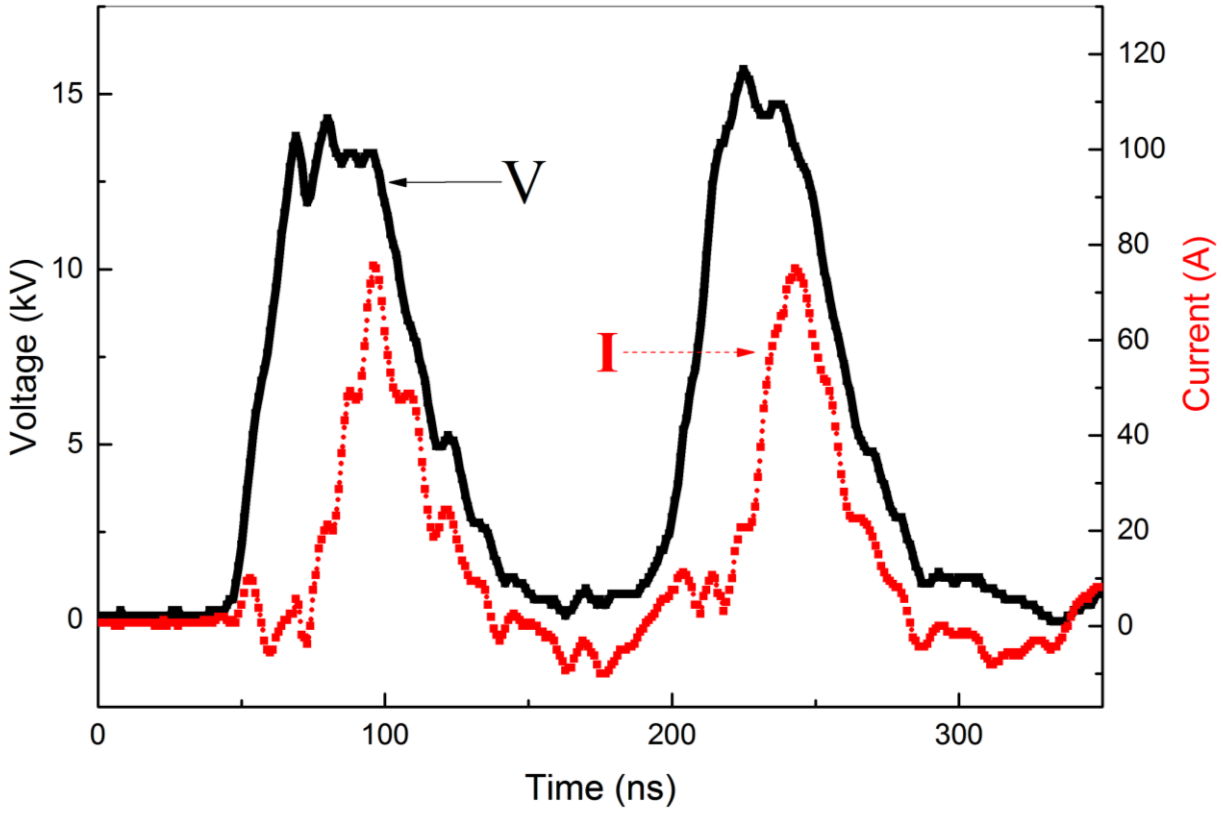

Fig. 5-4. Voltage and current waveforms for double pulse discharge with interval of 150 ns, for about same peak current obtained by a higher voltage of the second pulse.

5.2.3 Two Consecutive 15 kV, 50 ns Pulse in Different Time intervals

To find an explanation for this current leakage in the second pulse, these identical voltage pulses applied in different time intervals to observe the results.

In Fig. 5-5 time interval between pulses is 2 ms. In this case, current amplitudes are almost same. This is confirming that the initial states depend on the time. In the other words, in short time intervals some reasons are affecting the discharge process and cause a leakage in next pulses.

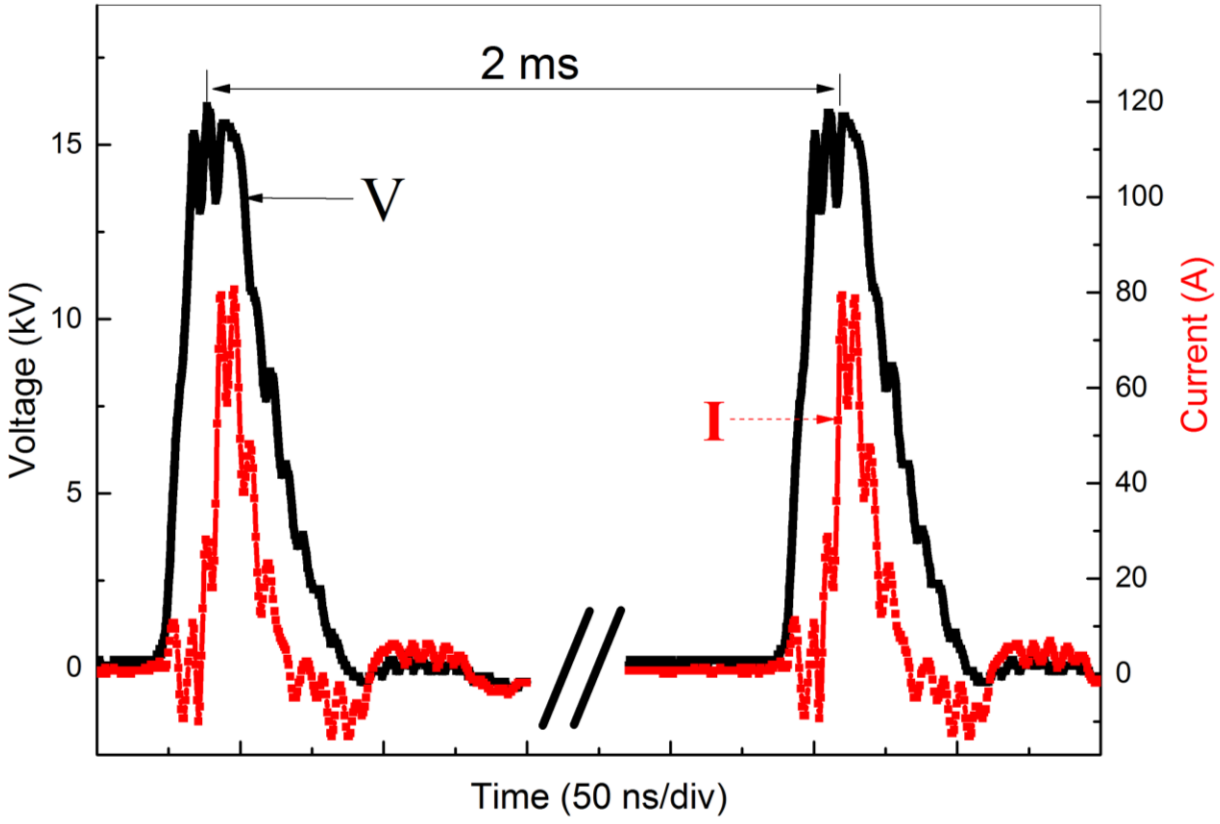

Fig. 5-5. Voltage and current waveforms for double pulse discharge with interval of 2 ms.

The results for different time intervals are summarized in Fig. 5-6, by comparing the peak current of two pulses. We can see that the current ratio (I2/I1) increased from ~0.55 to ~0.95 when the time interval is increased from 150 ns to 100 μs.

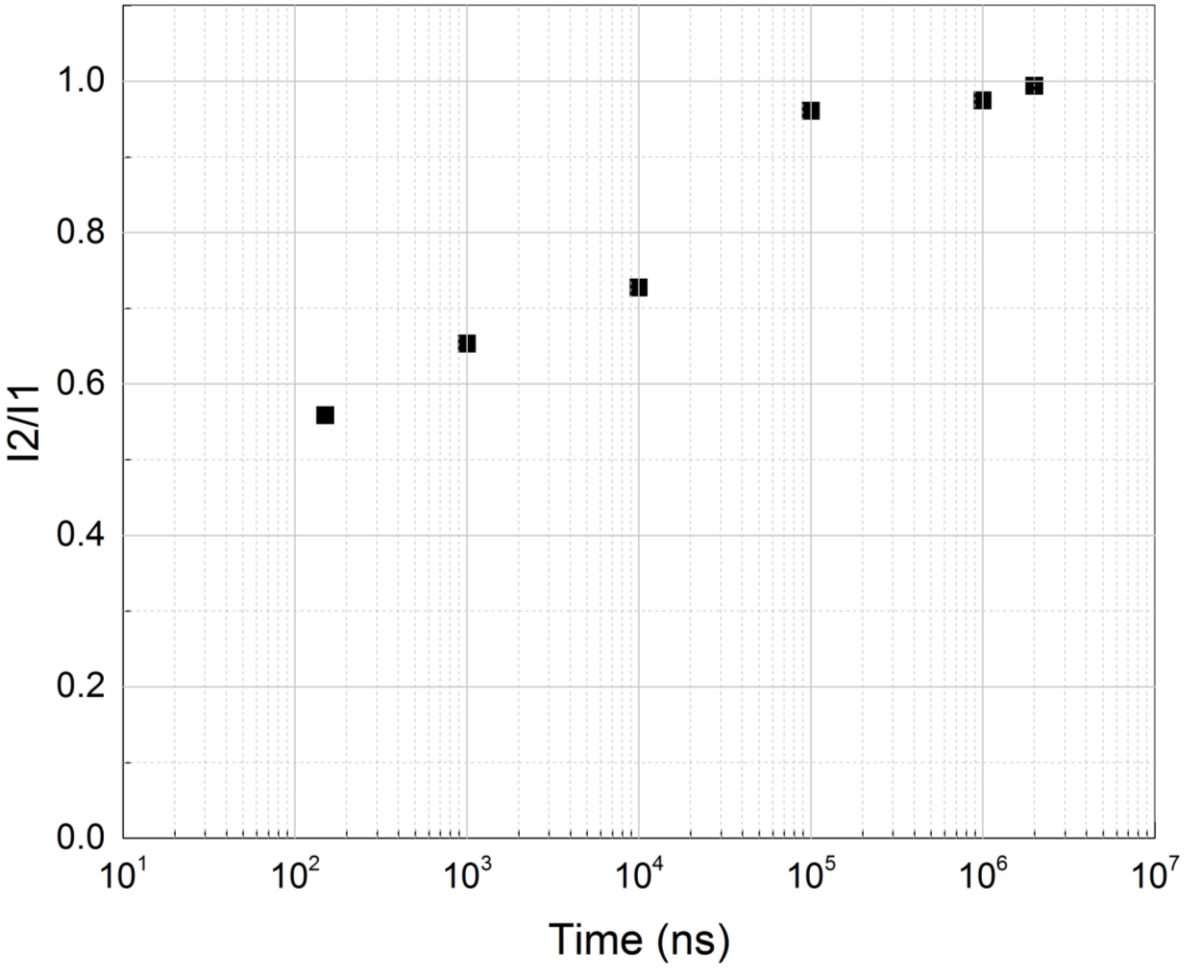

Fig. 5-6. Ratio of peak current of the second pulse to that of the first pulse, for different pulse intervals.

5.3 Physical Explanation

5.3.1 Discharge Process

Free electrons formed naturally in the inter-electrode space are accelerated towards the positive corona electrode by the electric field. In the vicinity of the high-voltage electrode surface, the electric field intensity reaches a critical level. Partial discharge initiates streamers that penetrate through the gas toward the cathode (pipe electrode), while the negative electrons carry the current to the anode (wire electrode). In this region, named ionization region, inelastic collisions of electrons and neutral gas molecules result in electrons breaking free of the molecules. This process creates free electrons and positive ions, which in turn are accelerated by the Coulomb force and produce further pairs of electrons and cations, in the so-called electron avalanche (Fig. 5-7).

By full development of streamers between the electrodes, the discharge phase transforms to a glow-like discharge with a large flow of current in the plasma channel produced by their propagation. In this case, discharge process can be categorized in two stages. The first one is the ‘streamer discharge’, in the other word ‘primary streamer’ discharge and it is followed by a ‘glow-like discharge’ which can be called also ‘secondary streamer’ discharge initiating by threshold voltage. The velocity of streamers increases with increasing applied voltage to the wire. Strong influence on the motion of the streamers head because of higher conductivity plasma channel between wire and streamers head can be a possible explanation [30].

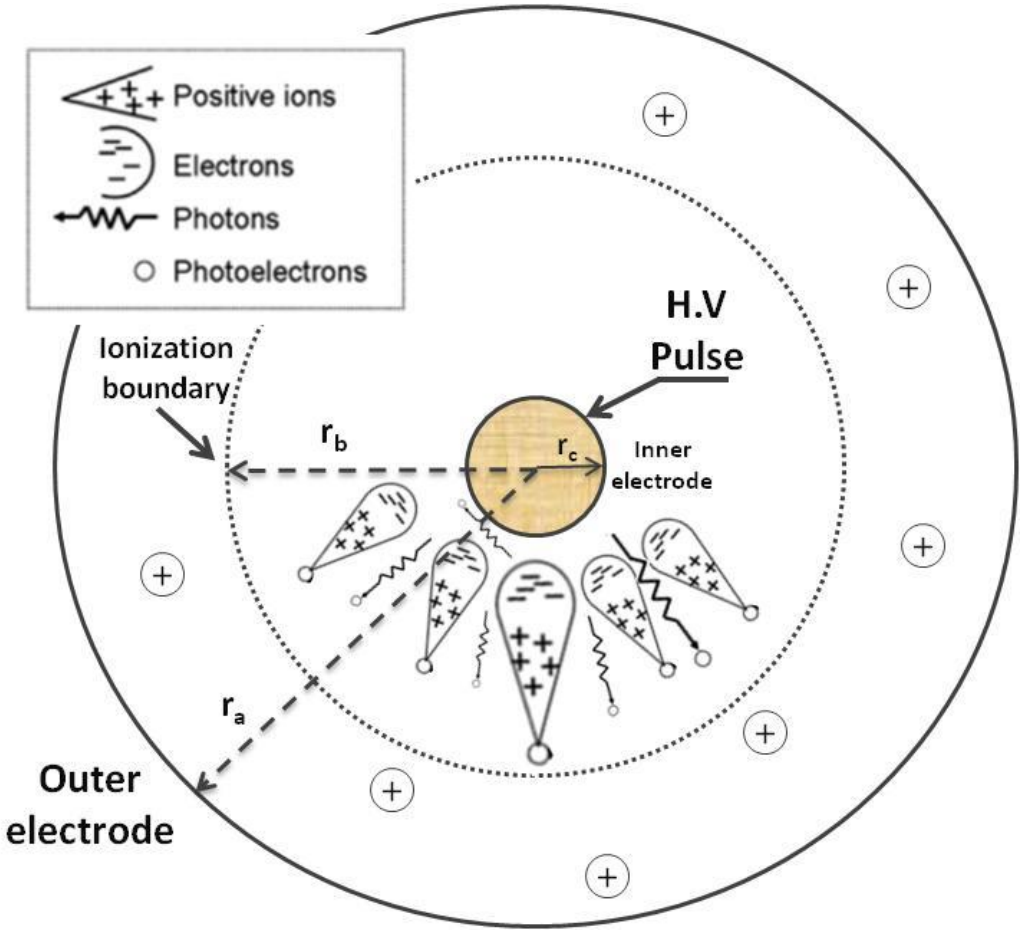

Fig. 5-7. Discharge process illustration in pulsed atmospheric discharge.

Near the corona electrode, electrons have average energies high enough to sustain their net production; however, at an increasing distance, the ionization rate decreases and the attachment rate increases. The location where the ionization rate equals the attachment rate defines the boundary of the ionization region. All newly produced electrons attach to molecules to form anions. This boundary lies very close to the high-voltage electrode. Beyond the ionization region, the field strength is insufficient to produce collision-induced electron-ion pairs and only ions of the same polarity as the corona electrode are present.

Depending on the type of energy supply and amount of energy transferred to the plasma, the properties of plasma change in term of electronic density or temperature. Pulsed power supply induces Non-local thermodynamic equilibrium plasmas. After the pulse, however, positive charges carried by the ions remain in the gas. A positive space charge due to the heavy and slow ions remains at the back. It has a very slow movement, especially because of rapidly decreasing applied field at the tip of the anode. This results in weakening of the resultant electric field in the region infront of the tip due to like polarity space charge at the positive electrode. They reside in the area where most of the discharge occurred, i.e. the area near the wire, until they dissipate by diffusion and recombination. It is the presence of this positive charge that may have caused the phenomena which we observed in the previous sections. In order to give a qualitative explanation, we have compared the electric field distribution for cases with and without the residual charge.

5.4 Qualitative Explanation by Designing a Model

This qualitative model is going to prepare a physical interpretation of current leakage phenomena in following pulses in a consecutive operation mode by comparing the electric field in different cases, without residual charges and with residual charges.

We calculate electric field in both cases and compare the effect of this residual charge.

5.4.1 Electric Field without Positive Residual Charge

In Fig. 5-8 our one-dimensional model for calculating the electric filed in this state is shown.

r_a . Wire radius
r_a . Iinner surface of pipe radius
r . Radius of calculated electric field

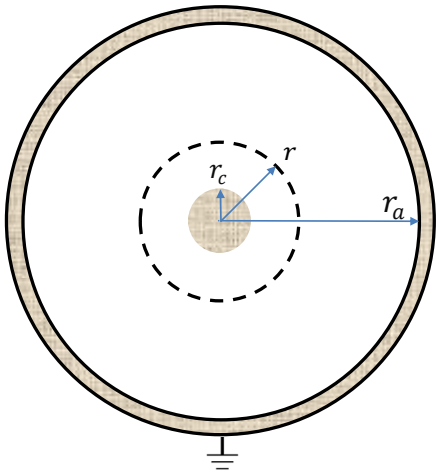

Fig. 5-8. One-Dimensional model for calculating the electric field before first pulse.

To find the needed density and field we need to consider.

- The connection between electric field and charge density

$$\nabla . E = \frac{\rho}{\varepsilon_0}$$

- Dependency of the field intensity from potential gradient

$$E = -\nabla\varphi$$

In case of wire inside and coaxial to a cylindrical collector, problem can be expressed in cylindrical coordinates as one-dimensional and all parameters depend only on radius. Which we can write.

$$\frac{1}{r}\frac{d(r.E)}{d_r} = \frac{\rho}{\varepsilon_0}$$

$$E = -\frac{d_\varphi}{d_r}$$

Considering no residual charges before the first pulse and positive voltage on the wire finally we reach to an equation for electric field and potential depend on the radius.

$$\rho = 0$$

$$\varphi(r_a) = 0$$

$$\varphi(r_c) = V_0$$

We can calculate the field:

$$\frac{1}{r}\frac{d(r.E)}{d_r} = 0$$

$$r.E = C_1, E = \frac{C_1}{r}$$

$$\varphi = -\int E\, d_r = -\int \left(\frac{\mathrm{C}_1}{\mathrm{r}}\right) d_r = -\mathrm{C}_1 \ln r + \mathrm{C}_2$$

$$0 = -\mathrm{C}_1 \ln r_a + \mathrm{C}_2$$

$$\mathrm{C}_2 = \mathrm{C}_1 \ln r_a$$

$$\varphi_{=} -\mathrm{C}_1 \ln r_{+} \mathrm{C}_1 \ln r_a = \mathrm{C}_1 ln \frac{r_a}{r}$$

$$V_0 = C_1 ln \frac{ra}{rc} \;\rightarrow = C_1 = \frac{V_0}{ln \frac{ra}{rc}}$$

$$\boldsymbol{E_{(r)} = \frac{C_1}{r} = \frac{V_0}{r ln \frac{ra}{rc}}}$$

$$\varphi_{(r)} = -\frac{V_0 lnr}{ln \frac{ra}{rc}} + \frac{ln_{ra}}{ln \frac{ra}{rc}} = V_0 \frac{ln \frac{ra}{r}}{ln \frac{ra}{rc}}$$

In Fig. 5-9 calculated electric filed in state of without of residual charges has been graphed.

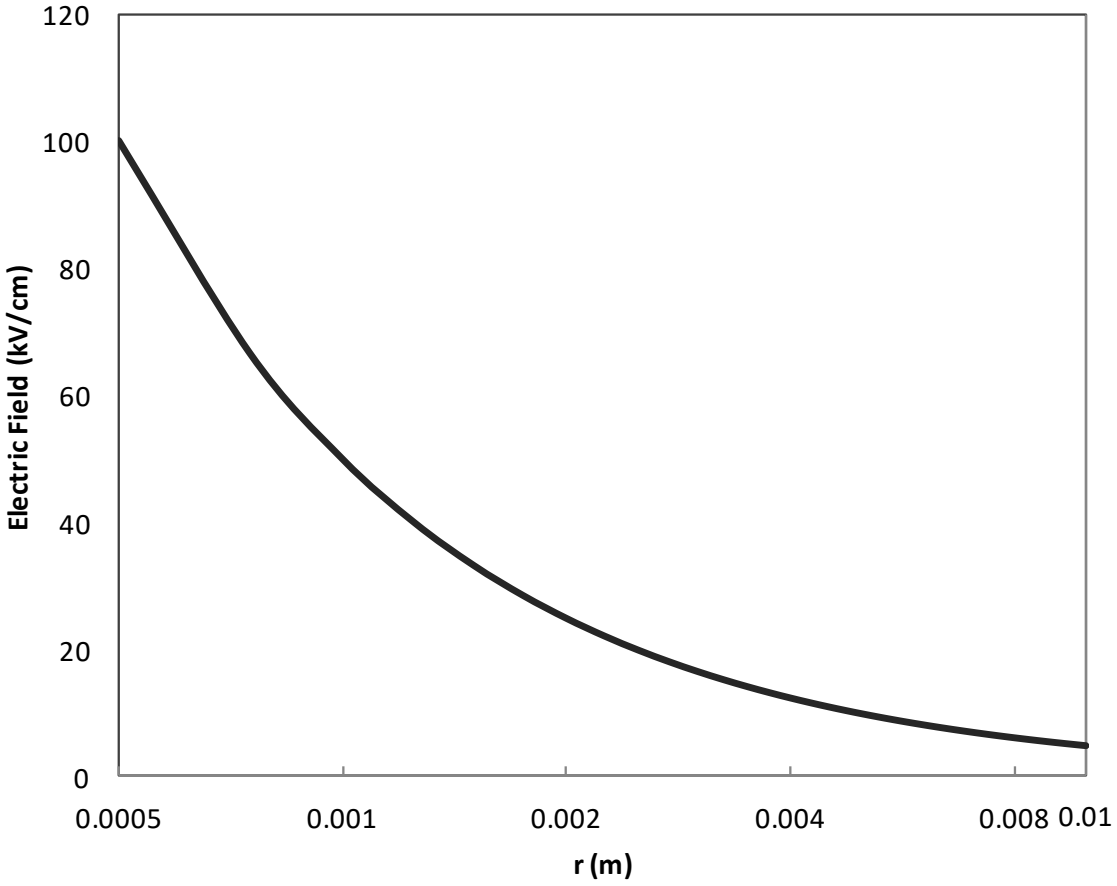

Fig. 5-9. Electric field when there is no residual charge before 1st pulse.

5.4.2 Electric Field with Positive Residual Charge

The model for the calculation is illustrated in Fig. 5-10 which shows the cross-sectional area between two electrodes. To represent the residual ions, we have added a layer of positive charge on the surface of the wire indicated as region 1 in Fig. 5-10 and the remaining volume between the gap is denoted as region 2. For simplicity, we assume the charge density is constant so that we can solve the one-dimensional Poisson equation analytically for given boundary conditions.

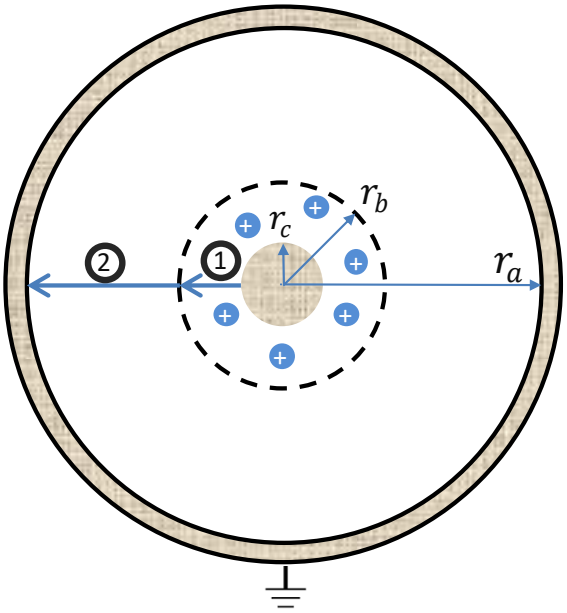

Fig. 5-10. One-dimensional model for calculating the electric field distribution between the electrodes, where ra,rb and rc are radii of pipe inner, residual charge layer and wire surfaces respectively. Regions 1 and 2 denote the regions with and without the residual charge.

We have to consider that, the pulse is too short that there is no time for the ions to follow the push of the applied electric field. Only the elections are sucked away by the positive electrode (the wire). In addition, the electrode configuration forms a very nonuniform electric-field distribution so that most of the charged particles are produced near the wire electrode. Because of that our model has a positive charge layer near the wire.

To calculate the electric field we have to consider the boundary conditions between region 1 and 2.

General conditions

$$\varphi(ra) = 0$$

$$\varphi(rc) = V_0$$

Boundary conditions

$$\varphi_{rb}^{1} = \varphi_{rb}^{2}$$

$$E_{rb}^{1} = E_{rb}^{2}$$

- **Region 2**

$$\boldsymbol{E = \frac{C_1}{r}}$$

$$\boldsymbol{\varphi = C_1 ln \frac{ra}{r}}$$

- **Region 1**

$$\boldsymbol{\rho \neq 0}$$

$$\mathbf{E} = \frac{\mathbf{r}\boldsymbol{\rho}}{\mathbf{2}\boldsymbol{\varepsilon_0}} + \frac{\mathbf{C_3}}{\mathbf{r}}$$

$$\varphi = \int E\, d_r = \int \left(\frac{\mathrm{r}\rho}{2\varepsilon_0} + \frac{\mathrm{C_3}}{\mathrm{r}}\right) d_r = \frac{\mathrm{r}^2\rho}{4\varepsilon_0} + \mathrm{C_3}\ln r + \mathrm{C_4}$$

$$V_0 = \frac{{r_c}^2\rho}{4\varepsilon_0} + \mathrm{C_3}\ln r_c + \mathrm{C_4}$$

$$\mathrm{C_4} = V_0 - \frac{{r_c}^2\rho}{4\varepsilon_0} - \mathrm{C_3}\ln r_c$$

For finding $C_3 and\, C_4$ constant we use the boundary conditions.

$$\varphi_{rb}^1 = \varphi_{rb}^2$$

$$\varphi_b = \mathrm{C_1} ln \frac{r_a}{r_b}$$

$$\mathrm{C_1} ln \frac{r_a}{r_b} = \frac{{r_b}^2\rho}{4\varepsilon_0} + \mathrm{C_3}\ln r_b + \mathrm{C_4}$$

$$\mathrm{C_4} = \mathrm{C_1} ln \frac{r_a}{r_b} - \frac{{r_b}^2\rho}{4\varepsilon_0} - \mathrm{C_3}\ln r_b$$

And considering:

$$E_{rb}^{1} = E_{rb}^{2}$$

$$\frac{C_1}{r_b} = \frac{r_b \rho}{2\varepsilon_0} + \frac{C_3}{r_b}$$

$$C_3 = C_1 - \frac{{r_b}^2 \rho}{2\varepsilon_0}$$

Then we use C4 equations to find the C1 and C3.

$$V_0 - \frac{{r_c}^2 \rho}{4\varepsilon_0} - C_3 \ln r_c = C_1 ln \frac{r_a}{r_b} - \frac{{r_b}^2 \rho}{4\varepsilon_0} - C_3 \ln r_b$$

Considering

$$C_3 = C_1 - \frac{{r_b}^2 \rho}{2\varepsilon_0}$$

$$V_0 - \frac{{r_c}^2 \rho}{4\varepsilon_0} - \left(C_1 - \frac{{r_b}^2 \rho}{2\varepsilon_0}\right) \ln r_c - C_1 ln \frac{r_a}{r_b} + \frac{{r_b}^2 \rho}{4\varepsilon_0} + \left(C_1 - \frac{{r_b}^2 \rho}{2\varepsilon_0}\right) \ln r_b = 0$$

By using this above equation we can find C1 and then C3.

The results are shown in Fig. 5-11. In the calculation, we have assumed that the ion layer has a total charge of 224 nC and a thickness of 3 mm.

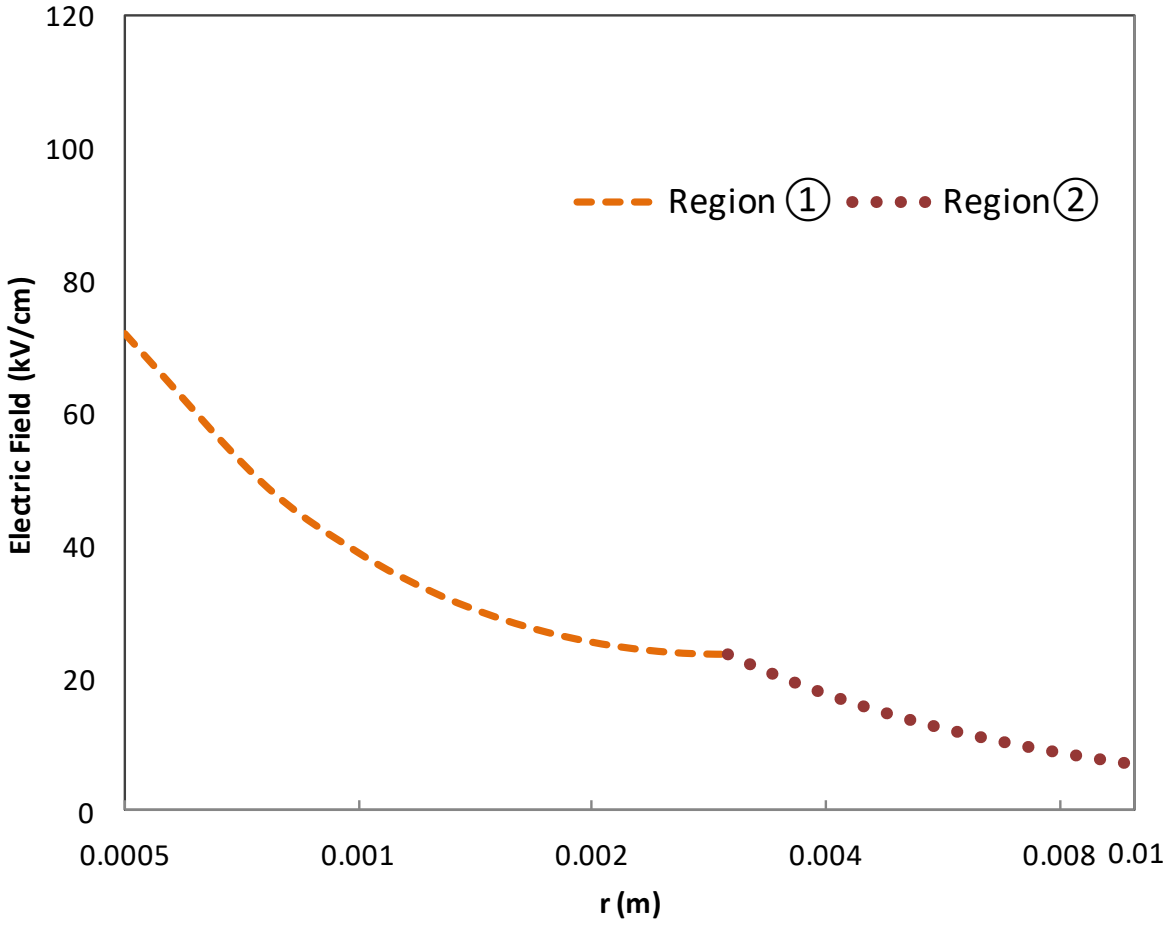

Fig. 5-11. Electric field calculation with residual charge.

5.4.3 Effect of Residual Charge on Electric Field

The calculation results shown in Fig. 5-12 indicate that the positive residual charge around the inner electrode (the anode) leads to a decrease of the electric field intensity near the wire electrode compared with that obtained without the residual charge. In other words, since the breakdown starts from the high-field area, the discharge threshold for the case without residual charge is lower than that with residual charge.

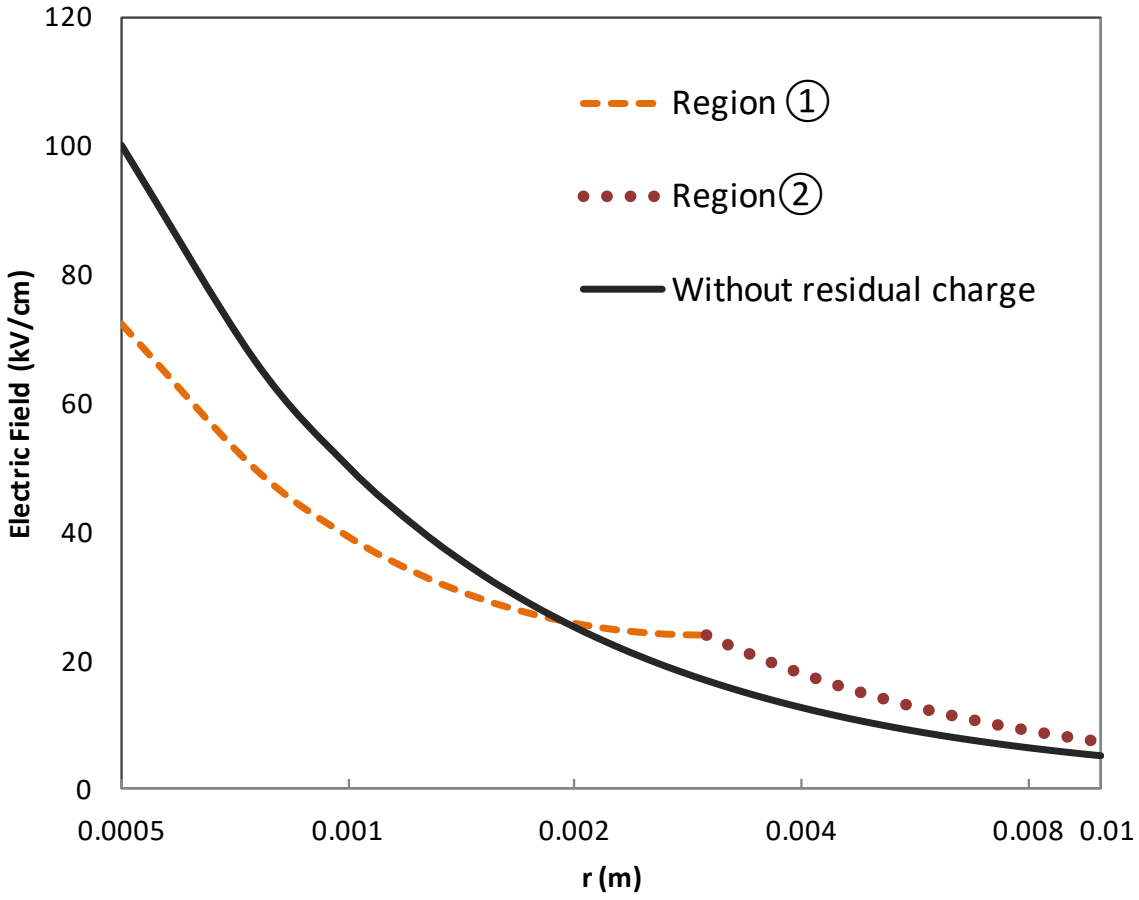

Fig. 5-12. Calculation results of radial electric-field intensity with and without the residual charge, for gap voltage of 15 kV.

Although this calculation cannot quantitatively explain the leakage current in short time intervals, it does offer a physical interpretation for the phenomena observed in the experiments.

Finally, if the phenomenon is indeed caused by the residual charge left by the previous discharge, the experimental results tell us that it takes approximately 100 μs for the residual charge to disappear before the second discharge gets back to normal.

First, in the calculation of Fig. 5-10, we have assumed a total charge of 224 nC in a cylindrical volume of radius 3 mm and length 320 mm. It corresponds to a particle density of ~ 10^{11} /cm^3, for single-charged ions. Considering the gas molecule density of ~ 10^{19} /cm^3 under atmospheric pressure, the average degree of ionization is therefore estimated to be on the order of 10^{-8}. Although this value is relatively low compared with most plasmas, the lack of negative electrons gives rise to strong space-charge induced electric field. This space-charge effect is the cause of the difference between two electric-field profiles shown in Fig. 5-12. Second, the thermal diffusion of the ions is heavily hampered by the high-density gas molecules. However, the ion drift velocity is proportional to the intensity of the electric field. Theoretically, ion drift velocity can reach the order of 10^6 m/s under an electric field of 10^4 V/cm which is the estimated space-charge field on the cylinder surface. Therefore, the ion expansion process is dominated by the electric field generated by the residual charge itself. Nevertheless, since the actual drifting is affected by many other factors, and the electric-field intensity depends very much on the location, quantitative solution for the drifting equations of the residual charge requires a complicated procedure.

6 CONCLUSION

- FPGA is a compact device with high capability for usage in Pulsed Power Technology.

- FPGA design has been studied, made and developed for different aspects of pulsed power energy like as pulse width modulation, pulse delay and pulse selection.

- Digital feedback by FPGA was conducted and was shown that due FPGA capabilities, very fast feedback process is achievable. In studied circuit delay was measured as 5 ns.

- LTD specification has been analyzed and FPGA and Pulse Generator usage in LTD has been compared. It is found that FPGA as compact, fast and having multiple outputs is absolutely better option for pulse output control of LTD.

- FPGA is used to provide control signal 1~30 different timing group and transferred to LTD. Results for 1, 3, 6, 10, 15, 30 groups of control signal with different timing has been analyzed and recorded. It is shown that with conducting different control signal FPGA arbitrary output in LTD is achievable.

- It was understood with increasing of groups of control signals with different timing power efficiency will decrease because of energy losses in magnetic core.

- LTD is expected to become a compact pulsed-power generator for industrial applications and LTD's ability in waveform control is shown by several experiments.

- We have used an LTD system consisting of 30 modules, each of them uses 24 power MOSFETs as switches. All LTD modules are controlled by an FPGA board so that each module can be switched ON and OFF at arbitrary timings defined by the FPGA clock.

  The large number of modules and their arbitrary switching times allow us to shape the output voltage waveform by using proper control signals. This is important for applications where the performance is sensitive to the waveform, such as pulsed atmospheric discharge.

- We have reported a demonstration experiment for waveform control of a discharge load driven by LTD. The experimental results show that, by properly adjusting the applied voltage, the discharge current behavior can be controlled, to a certain extent, so that we can keep the current value near 10, 20, 30, or 40 A. We can also force the current to jump from one of these values to another, during the pulse.

- Pulsed atmospheric discharge has been studied by using a coaxial discharge load consisting of a wire and a metal pipe, without dielectric barrier between them. Special attention has been paid to the current amplitude when high-voltage pulses are applied to the electrodes. The high-voltage pulses have been generated by

using an LTD-type pulsed voltage generator which is known for its output flexibility. The experimental results have indicated that, when two consecutive pulses are applied, the peak current associated with the second pulse is clearly smaller than that of the first pulse, especially for the cases with pulse interval less than 100 μs. This phenomenon is not observed when the pulse interval is increased to 2 ms. It looked as if the first pulse has left some kind of effect in the gas that ceases in less than two milliseconds.

- In order to provide a physical interpretation of this effect, we have looked into the influence of residual positive charge that is created and littered in the gas by the first discharge. A one-dimensional model has been built in order to solve for the electric field distribution. The calculation results have indicated a significant drop of the electric field when the residual charge has been taken into account, offering a qualitative explanation for the experimental results.

  In other words, it can be physically interpreted that the first pulsed discharge has left some positive charge in the gas that plays a role in weakening the electric field when the second pulsed voltage is applied. The discharge load we have used has a typical corona discharge configuration, where the electric field distribution is extremely nonuniform.

  When the voltage is applied, the initial breakdown occurs only in a limited volume where the field intensity is above the threshold. The discharge creates large amount of charged particles, positive ions and negative electrons, in the gas

while electrons are quickly removed by the electric field generating an electric current. However, the positive ions remain in the gas for a much longer time than that of electrons. This research has indirectly provided an experimental evidence for the existence of the positive residual charge.

- This research has presented a phenomenological study for pulsed discharge under atmospheric pressure.

7 FUTURE WORK

- Automatic feedback system for waveform control of LTD considering load characteristics.

- Study on longer or negative pulses and carry out the experiments to analyze the pulse leakage phenomena in the second pulse.

- Study on how to reduce the effect of residual positive charges in on the second pulse.

8 PUBLICATION

Journal papers:

- M. R. Kazemi, T. Sugai, A. Tokuchi, W. Jiang, “Waveform Control of Pulse-Power Generator based on Solid-State LTD,” IEEE Trans. Plasma Sci., vol. 45, no.2, pp. 247-251, Feb. 2017.

- M. R. Kazemi, T. Sugai, A. Tokuchi, W. Jiang, “Study of Pulsed Atmospheric Discharge Using Solid-State LTD,” IEEE Trans. Plasma Sci., vol. , no., pp. 1-5, May. 2017.

Conference Papers:

- M.R. Ghurbanali, H. Sugiyama T. Sugai, A. Tokuchi, W. Jiang, “Pulse output control of LTD by using FPGA,” Proceeding 5th Euro-Asian Pulsed Power Proceeding no. 2, pp.294-297, Kumamoto, Japan, Sep, 2016.

- M.R. Ghurbanali, T. Sugai, A. Tokuchi, W. Jiang, “ Waveform Control of Pulsed Corona Discharge ,” Proceeding 21st International conference on gas discharge and their applications no. 2, pp.537-540 Nagoya, Japan, Sep. 11-16, 2016.

9 REFERENCES

1. Bluhm, H, Pulsed Power: Principles and Applications, Springer-Verlag, Berlin Heidelberg, 2006.

2. Lambert M. S, Mariam T. T, Susan F.H, Pulsed Power, Betascript, 2011.

3. W. Jiang, "Solid-State LTD Module Using Power MOSFETs" IEEE Trans. Plasma Sci, VOL. 38, NO.10, pp. 2730-2733, Oct 2010.

4. W. Jiang and A. Tokuchi, "Repetitive linear transformer driver using power MOSFETs," IEEE Trans. Plasma Sci., vol. 40, no. 10, pp. 2625–2628, Oct. 2012.

5. W. Jiang, H. Sugiyama, and A. Tokuchi, "Pulsed power generation by solid-state LTD," IEEE Trans. Plasma Sci., vol. 40, no. 11, pp. 3603–3608, Nov. 2014.

6. J. D. Cobine, Gaseous Conductors, New York: Dover, 1958.

7. J. Millman, S. Seely, Electronics, Chapters 9, 10 and 11, New York: McGraw-Hill, 1951.

8. G. Herzberg, Atomic Spectra and Atomic Structure, New York: Dover, 1944.

9. W. Middleton, M. E. Van Valkenburg, Reference Data for Engineers: Radio, Electronics, Computers and Communications, p. 16-42, Newnes, 2002.

10. J. Dakin, R. Brown, Handbook of optoelectronics, Volume 1, p. 52, CRC Press, 2006.

11. D. R. Reyes, M. Ghanem, G. M. Whitesides, A. Manz, Glow discharge in microfluidic chips for visible analog computing, Lab on a Chip. 2, p. 113–6, 2002.

12. "Glow discharge in microfluidic chips for visible analog computing". Nature. 27 May 2002. doi:10.1038/news020520-12.

13. C. Tendero, C. Tixier, P. Tristant, J. Desmaison, P. Leprince, "Atmospheric pressure plasmas: A review," Spectrochimica Acta Part B: Atomic Spectroscopy,. vol. 61, no. 1, pp. 2-30, 2006.

14. W. Hartmann, M. Roemheld, K. Rohde, F.J. Spiess, “Pulsed Corona in Water: Pulse Generation and Applications,” Plasma Science, IEEE 34th ICOPS, Albuquerque, NM, USA, June 2007.

15. M. Goldman, A. Goldman, R. S. Sigmond, “The Corona Discharge, Its Properties and Specific Uses ,” Pure Appl. Chem., vol. 57, no. 9, pp. 1353-1362, 1985.

16. J.S Chang, P. A. Lawless, T. Yamamoto, “Corona Discharge Process,” IEEE Trans. Plasma Sci., vol. 19. no. 6, pp. 1152–1166, 1991.

17. K.H. Schoenbach, U. Kogelschatz, K.H. Becker, R.J. Barker, Non-Equilibrium Air Plasmas at Atmospheric Pressure, chaoter 1, UK, 2007.

18. S. Nijdam, E.Veldhuizen, P. Bruggeman, U. Ebert, Plasma Chemistry and Catalysis in Gases and Liquids: An Introduction to Nonequilibrium Plasmas at Atmospheric Pressure, chapter 1, John Wiley & Sons, Ltd, 2012.

19 . J. Wei, M. Denn, J. H. Seinfeld, A. Chakraborty, J. Ying, N.Peppas, G. Stephanopoulos, Molecular Modeling and Theory in Chemical Engineering, Academic Press, 2001.

20. G.I. Font. “Boundary Layer Control with Atmospheric Plasma Discharges,”, AIAA Journal, Vol. 44, No. 7, pp. 1572-1578, 2006.

21. K.C. Leou , G.S. Chen, C. Lin, T.L. Lin, C.H. Tsai, “Measurement of time varying RF impedance of a pulsed inductively coupled plasma,” ICOPS. IEEE Conference Record, Banff, Alberta, Canada, 2002.

22. T. Yokoo, K. Saiki, K. Hotta, W. Jiang, “Repetitive Pulsed High-Voltage Generator Using Semiconductor Opening Switch for Atmospheric Discharge,” IEEE TRANSACTIONS ON PLASMA SCIENCE, VOL. 36, NO. 5, OCTOBER 2008.

23. M. van Heesch, Sander S. V. B. van Paasen, “Pulsed Power Corona Discharges for Air Pollution Control” IEEE TRANSACTIONS ON PLASMA SCIENCE, VOL. 26, NO. 5, OCTOBER 1998.

24 . http://tmms.co.jp/EFD/Links_&_related_topics/The_lifters_dedicated_page.htm Accessed. 10 May 2017.

25. R. Gilles, K.D. Weltmann, E. Schade, M. Claessens, “ Determination of the Residual Charge after Current Extinction-An Integral Approach,” Proc. IEEE,. vol. 2, pp. 481 - 484, Sep .2000.

26. H. Höft, M. Kettlitz, M. M Becker, T. Hoder, D. Loffhagen, R. Brandenburg, K.D. Weltmann, “Breakdown Characteristics in Pulsed-Driven Dielectric Barrier Discharges: Influence of the Pre-Breakdown Phase Due to Volume Memory Effects,” Journal of Physics D: Applied Physics,. vol. 47. no. 46, Oct. 2014.

27. S.T. Chun, “Spatial and Temporal Evolution of a Pulsed Corona Discharge Plasma,” Journal of the Korean Physical Society, Vol. 33, No. 4, pp. 428-433, October 1998.

28 . Altera Measurable Advantage (1995-2014) FPGA. Available at http. //www.altera.com/products/fpga.html (Accessed. 20 April 2013).

29. DE0_Nano_SoC_User_Manual.

30. D. Z. Pai, G. D. Stancu, D.A. Lacoste, C. O. Laux, “Nanosecond Repetitively Pulsed Discharges in Air at Atmospheric Pressure-The Glow Regime,” Plasma Sources Sci. Technol,. vol. 18, no. 4, pp. 1-7, Oct. 2009.